The
ENGINEERS' DIGEST

REVIEW OF ENGINEERING PROGRESS ABROAD

JUL 1 1 1945

VOL. VI. No. 5 MAY, 1945

ERING
ARY

In addition to all their other advantages, CHURCHILL Precision Roll Grinders are easily operated.

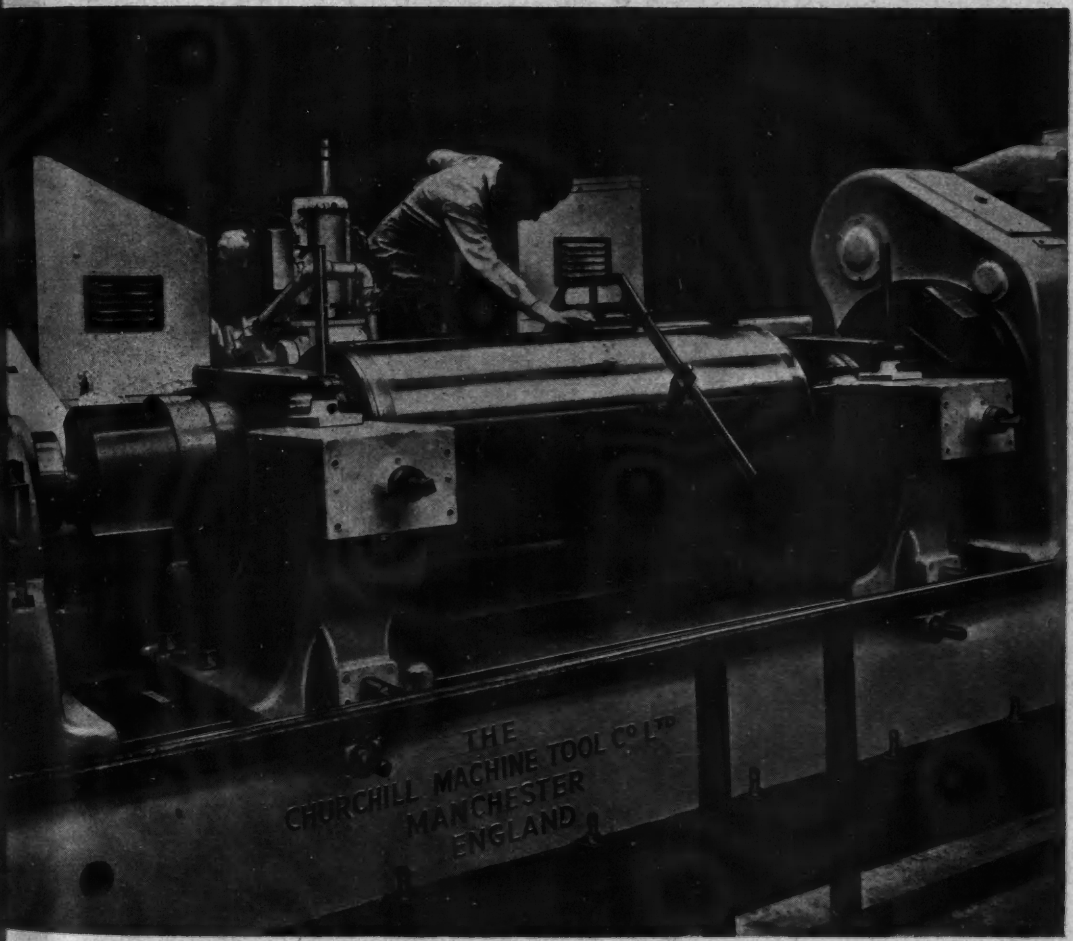

THE CHURCHILL MACHINE TOOL CO. LTD., BROADHEATH, Nr. MANCHESTER.

THE ENGINEERS' DIGEST

REVIEW OF ENGINEERING PROGRESS ABROAD

Published Monthly at 120, Wigmore Street, London, W. 1.

Publishers : **ENGINEERS' DIGEST LTD.** – – – – – – Telephone : WELBECK 9357

Adverstisement Dept. – 120, Wigmore Street, London, W.1. – – Telephone : Welbeck 9357

Distribution – – E. & F. N. SPON, LTD., 57, Haymarket, London, S.W.1.
Telephone : Whitehall 1860. Telegrams : Fenspon, Lesquare, London

Editorial Dept. – – 120, Wigmore Street, London, W.1. – – Telephone : Welbeck 9357

Subscriptions to : ENGINEERS' DIGEST LTD., 120, Wigmore Street, London, W.1, or
E. & F. N. SPON, LTD., 57, Haymarket, London, S.W.1.

ANNUAL SUBSCRIPTION OF 12 NUMBERS, £2 2s. **SINGLE COPIES, 4s. 6d.**

ADVISORY COMMITTEE

J. F. ALCOCK, B.A., A.M.I.Mech.E.
R. W. ALLOTT, M.A., A.R.Ae.S.
E. ALTON, D.Eng., A.M.Inst.B.E.
H. H. ASBRIDGE, M.B.E., M.I.Mech.E.
R. W. AYERS, M.I.W.
Col. J. BOWDEN, M.Inst.C.E., M.I.Mech.E.
H. H. BROUGHTON, M.I.Mech.E.
F. BUCKINGHAM, B.Sc., A.M.Inst.C.E., A.M.I.Mech.E.,
T. H. BURNHAM, B.Sc. (Lond.), A.M.I.Mech.E. [A.M.I.E.E.
J. S. CASWELL, M.Sc., M.I.Mech.E.
G. C. SAFFERY COOPER.
J. DICK, Ph.D., B.Sc., A.M.I.Mech.F.
D. FIFE, M.I.Mech.E.
G. E. FOXWELL, D.Sc. (Lond.), F.Inst.P., F.Inst.F.,
R. GRIFFITHS, M.Sc. [M.Inst.Gas.E.
H. HEYWOOD, Ph.D., M.Sc. (Eng.), A.M.I.Mech.E.
O. HURST, M.Inst.N.A.
Capt. J. S. IRVING, M.I.Mech.E., M.I.A.E., A.F.R.Ae.S., M.S.A.E.
F. C. JOHANSEN, M.Sc. (Eng.), M.I.Mech.E., F.R.Ae.S., M.I.Loco.E.
W. J. KEARTON, D.Eng., M.I.Mech.E., A.M.Inst.N.A.
Prof. W. KERR, Ph.D., M.I.Mech.E.
G. V. LOMONOSOFF, Dr.Ing, M.I.Mech.E.
B. J. LYMER, M.I.Mech.E.
D. T. MacIVOR, M.I.Mech.E., M.Cons.E.
W. O. MANNING, F.R.Ae.S.
R. B. MATTHEWS, Wh.Ex., A.M.Inst.C.E., M.I.E.E., F.R.Ae.S.
Prof. A. L. MELLANBY, D.Sc., LL.D., M.I.Mech.E.
J. H. R. RATCLIFFE, B.Sc. (Eng., Hons.), M.I.Mech.E.
Col. C. W. D. ROWE.
W. A. SCOBLE, D.Sc., A.R.C.Sc., M.I.Mech.E.
P. W. SEEWER, D.E. (Zurich), M.Inst.C.E., M.I.Mech.E.
Prof. S. PARKER SMITH, D.Sc., M.I.E.E., A.M.Inst.C.E.
C. F. H. VERITY, A.M.Inst.C.E., A.M.I.E.E., A.M.I.Mech.E.
E. G. WALKER, F.C.G.I., B.Sc. (Eng.), M.Inst.C.E., M.I.Mech.E., M.Am.Soc.C.E.
Major F. L. WATSON, M.Inst.C.E., M.I.Mech.E.
G. WATSON, M.Inst.C.E., M.I.Mech.E.
C. H. WOODFIELD, M.I.Mech.E., M.I.Struct.E.
T. WRIGHT, Ph.D., M.Sc.
M. L. YATES, Ph.D., M.Sc.Tech., M.A. (Com.), M.I.Mech.E.

CONTENTS

page

A Novel Automatic Synchronizer 136
" *The Engineers' Digest*," *Vol.* 6, *No.* 5, *p.* 136.

Appropriate Method for Finding the Shear Centre Position of a Single Cell Wing Nose Beam .. 130
" *The Engineers' Digest*," *Vol.* 6, *No.* 5, *p.* 130.

Carrying Capacity of Bearing Liners of Sintered Iron 113
" *The Engineers' Digest*," *Vol.* 6, *No.* 5, *p.* 113.

Comparison between the Different Methods of Regulation of Electrically Driven Turbo-Blowers for Steelworks 114
" *The Engineers' Digest*," *Vol.* 6, *No.* 5, *p.* 114.

Diesel Fuels 131
" *The Engineers' Digest*," *Vol.* 6, *No.* 5, *p.* 131.

Investigation of the Isothermal Viscosity of Bearing Alloys 127
" *The Engineers' Digest*," *Vol.* 6, *No.* 5, *p.* 127.

Novel Photoelectric Pyrometer 119
" *The Engineers' Digest*," *Vol.* 6, *No.* 5, *p.* 119.

Pressure Losses in Branches of Square Channels 124
" *The Engineers' Digest*," *Vol.* 6, *No.* 5, *p.* 124.

Temperature Distribution and Heat Flow in Bars 122
" *The Engineers' Digest*," *Vol.* 6, *No.* 5, *p.* 122.

Temperature Measurement of Air and Gases at High Velocity of Flow 137
" *The Engineers' Digest*," *Vol.* 6, *No.* 5, *p.* 137.

The Motion Resistances of Railway Vehicles and the Tractive Resistance of the Brown Boveri Gas Turbine Locomotive 133
" *The Engineers' Digest*," *Vol.* 6, *No.* 5, *p.* 133.

A NEW DEVELOPMENT IN ARC WELDING

THE POLYTRODE

PATENTS APPLIED FOR

FOR THE WELDING OF:—

Thin Gauge Mild Steel.
Aluminium and its Alloys with A.C.
Ferrous and Non-Ferrous Alloys by the Carbon Arc Process.

Can be used with any Standard D.C. or A.C Welding Plant.

Write for particulars to—

ACTARC SUREARC

ARC MANUFACTURING CO., LTD.
PROPRIETORS OF THE SURE-ARC ELECTRODE CO., LTD.
ACTARC WORKS, GOLDHAWK ROAD, LONDON W.12.
TELEPHONE: SHE 1151 TELEGRAMS: ACTIVARC, PHONE, LONDON. CABLES: ACTIVARC, LONDON.

REGD. TRADE MARK

3746

ESC
SMALL
TOOLS
We hold large stocks of all regularly use Milling Cutters, Reamers Butt Welded Tools, Tool Bits and "Escaloy" Cemented Carbide Tipped Tools for high speed cutting.
ENGLISH STEEL CORPORATION LTD
OPENSHAW — MANCHESTER

CARRYING CAPACITY OF BEARING LINERS OF SINTERED IRON.

By E. HEIDEBROEK. (From *VDI Zeitschrift*, Vol. 88, Nos. 15/16, 1944, pp. 205-207).

SINTERED iron has come to be used as a favourite metal for bearing liners mainly because of its porosity which makes possible the retention of a certain amount of oil in its innumerable pores by capilliary force. Rising temperature causes the metal to sweat, thereby maintaining a continuously lubricated surface for a considerable length of time. Bearings of this kind, which are known as the self-lubricating type, are preferably employed where a regular external supply of lubricant is difficult to maintain. Heretofore little was known, however, about the carrying capacity of sintered iron liners and about the interrelationship between carrying capacity, and of such factors as structure of the material, kind and quantity of the lubricant, surface quality, and other factors.

From the viewpoint of the hydrodynamic theory of lubrication, sintered iron liners would not be expected to produce particularly favourable results, since this theory demands a perfectly smooth ideal surface as prerequisite. In fact, no matter how carefully a sintered metal may have been machined, in micro-geometric respects it will always have a highly pitted surface in which the molecular chains are unable to find that anchorage normally required for the establishment of an unbroken oil film. No doubt, where high speeds are involved, this type of surface will have an unfavourable effect. Indeed, the test results related hereunder show clearly that the field of successful application lies within the range of low speeds with an upper limit of 5 m. per sec. at most. If higher speeds are employed, the running qualities of the sintered metal bearing will approximate to that of an ordinary bearing of rather mediocre quality. And even this result will only obtain if a continuous supply of lubricant is ensured as in any ordinary bearing.

The outstanding quality of sintered iron bearings is therefore characterised by the fact that such bearings are capable of highly successful, long time operation with a low coefficient of friction and without any external oil supply, provided that they are operated at low temperature with the loading not exceeding a certain value.

The physical mechanism of this kind of "static" condition of lubrication cannot be explained on the basis of the general hydrodynamic theory and is still to be investigated Nor can it be assumed that through the capilliaries a sufficient flow of lubricant from regions of higher pressure to such of lower pressure takes place, particularly if the extremely small flow velocity is considered Moreover, no oil is discharged through the bearing clearance. In spite of this, there persists a molecular layer of lubricant on the liner surface capable of carrying considerable loads. But, as mentioned before, this molecular layer is sensitive to increases in the temperature as well as to increases in the peripheral speed of the journal; and it was found that in these respects the structural condition of the liners is of considerable influence.

A bearing testing machine was employed to carry out comparative tests on a journal of 60 mm. diameter and 40 mm. width, the bearing clearance amounting to 0.25 mm. (Fig. 1). In the test runs carried out with full lubrication, a standardised oil of about 5 degrees Engler at 50 deg. C. was supplied to the liners at a pressure of 1 atm. g. at 20 deg. C.; whilst in the case of drip feed, the rate of oil supply could be adjusted at some 10 drops per minute, the oil supply being completely shut off towards the end of the test run. Each test run was preceded by a preliminary run of several hours under load with continuous lubrication in order to establish equilibrium conditions.

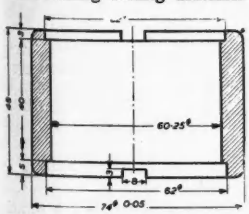

Fig. 1. Dimensions of sintered iron liners tested.

The temperature of the oil film at a point in front of the pressure apex was measured by means of a thermocouple, and speed of the journal and the turning moment of the liner were also recorded in order to determine the friction factors. All tests were made under equilibrium conditions. The maximum bearing loadings were determined for different journal speeds, this loading limit being defined as the highest load that could be carried without jeopardizing quiet running of the bearing and without exceeding an oil film temperature of 80 deg. C. Under these conditions neither measurable wear nor contact friction were incurred. All test runs were made with one and the same ground shaft of St. 70.11 material (0.6 C. steel of 70–85 kg./mm² UTS).

The results of the test runs are indicated in Figs. 2–6. In all cases, except one, the liners had been made of sintered Hametag iron powder, which is a mechanically powdered product. The liners had been supplied by various expert manufacturers in the field; and, as will be seen from the figures, considerable variations existed in the density and granulation of the finished product.

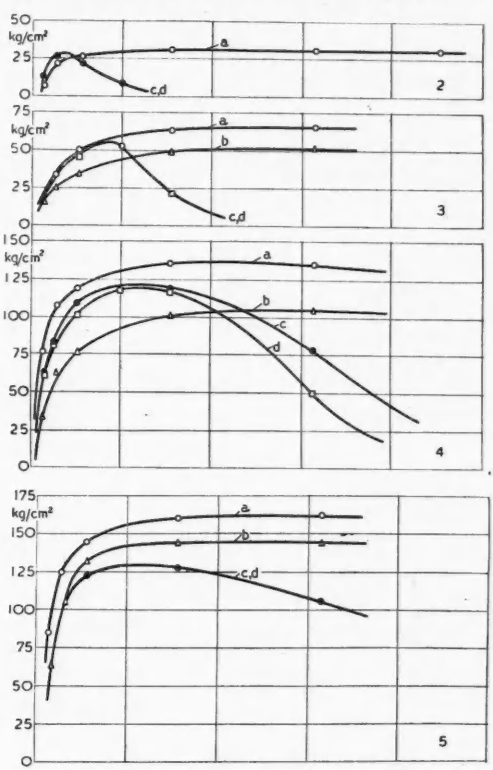

Figs. 2-5 (See captions on next page)

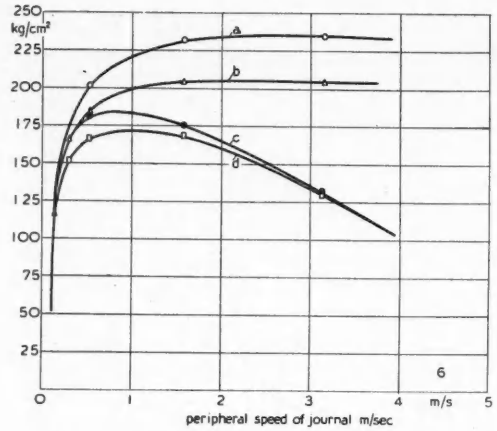

Figs. 2-6. **Bearing pressure *versus* peripheral speed characteristics of different liners of sintered iron powder.**
(a) Continuous lubrication after extended initial run.
(b) Continuous lubrication after 3 hr. initial run.
(c) Lubrication by drip oiling.
(d) Without supply of lubricant from external source.

Fig.	Powder	Granulation	Density g/cm3	Machining by	Additions
2	Hametag	coarse	5.8	lathe	—
3	Chemically produced	" special "	5.1	"	lead
4	Hametag	fine	5.8	"	—
5	Hametag	fine	5.8	"	—
6	Hametag	medium	6.4	size-broach	—

The test results charted in Figs. 4, 5 and 6 must be considered excellent. The specific loadings attained with these liners show that within the speed range indicated even high quality bearing metals may be replaced by sintered iron. Liners of the type shown in Fig. 5 are seen to combine high load carrying ability in the case of continuous lubrication with a particularly wide range of load carrying ability under conditions of intermittent lubrication. The shortcoming of the other liners in the latter respect is evident in the graphs concerned.

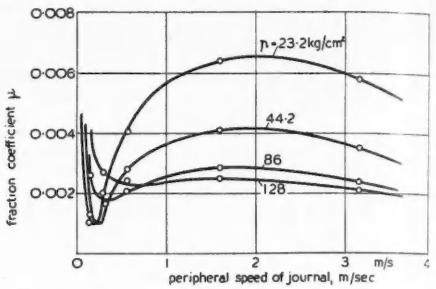

Fig. 7.
Friction coefficients obtained with liner Fig. 5.

In Fig. 7 are charted the friction coefficients obtaining with the liner referred to in Fig. 5, which refers solely to conditions of continuous lubrication. It will be seen from this graph that subsequent to the point of inflection the friction coefficients rise to maximum values in the manner of " hydrodynamic " curves. Once these maxima are exceeded, a slight decline in the respective friction coefficient occurs, this decline being probably due to an increase in the temperature of the oil film. In all cases, however, the bearing temperatures remained low, rarely rising to 60 deg. C.

Taken as a whole, the numerous investigations show the fundamental fact that the main qualities are determined by the degree of porosity and the fineness of granulation, that is to say, the porosity must not exceed a certain degree, or *vice versa* the density must not fall below a certain limiting value. However, neither an excessively high density chosen for the sake of mechanical strength nor an excessively fine granulation offer any advantages, but there exists a combination of values which ensures optimum bearing characteristics from the aspects of high carrying capacity under regular operating conditions and safety of operation under emergency conditions, such as insufficient lubrication.

That such optimum characteristics can actually be obtained is demonstrated by the graphs Figs. 4–6. On the basis of the large number of tests made, it has been found possible to establish definite rules to be followed in the choice of the desired product. However, the question why success is dependent upon the choice of certain microstructures, is still awaiting an answer.

COMPARISON BETWEEN THE DIFFERENT METHODS OF REGULATION OF ELECTRICALLY DRIVEN TURBO-BLOWERS FOR STEELWORKS.

By M. HALLER (Hv.). (From *The Brown Boveri Review*, Nov.–Dec., 1943, pp. 328-336)

BOTH pressure and quantity of the blast air must be capable of being quickly adapted to the varying conditions of the blast period during the treatment of pig iron by the Bessemer or Thomas processes. Moreover, since the powers absorbed by steelworks blowers are usually very large, it is very important that the efficiency of the blower set shall be high throughout the operating regulation range.

THE RESISTANCE CHARACTERISTIC OF THE CONVERTER PLANT.

The resistance which the compressor has to overcome in order to force the required air quantity through the converter is constituted by the sum of the resistances of the liquid metal and of the flow friction. The head of liquid of the molten iron offers an approximately constant resistance to the air, independently of the air quantity. In the present study the head of liquid is assumed to be between 650 and 700 mm., corresponding to a pressure on the converter base of about 0.5 kg./cm² gauge. The resistance of the tuyères and of the piping varies practically as the square of the delivery quantity. The back-pressure curve of the blower is, therefore, a parabola, with the origin at a height given by the height of the head of liquid. The comparison of the different methods of regulation discussed below is based on such a characteristic. During the tilting of the converter, the resistance characteristic is somewhat lower; as however the duration of the tilting operation is relatively short, this has been neglected in the following.

METHODS OF REGULATING THE COMPRESSOR.

The alternative methods of regulation of a centrifugal compressor are best seen with the aid of the following relation.

Let

H = Delivery head of the compressor in metres of liquid or of gas column, m.
g = Acceleration due to gravity, m/s².
u_1, u_2 = Peripheral velocity of the impeller blading at the inlet and outlet respectively (Fig. 7 B–E), m/s.
c_{u1}, c_{u2} = Tangential components of absolute inlet and outlet velocities of the medium delivered (Fig. 7 B–E), m/s.
γ_m = Average specific weight of the medium during compression in kg./m³.
P_1 = Absolute suction pressure of the blower in kg./m².
P_2 = Absolute delivery pressure of the blower in kg./m².
P_V = Pressure loss in the impeller and diffusor in kg./m².

According to Euler :

$$H = \frac{1}{g}(u_2\, c_{u2} - u_1\, c_{u1}) \quad .. \quad .. \quad .. \quad (1)$$

The increase in pressure produced by the above is :

$$P_2 - P_1 = \gamma_m \,.\, H - P_V \quad .. \quad .. \quad (2)$$

Combining these, the absolute delivery pressure is given by :

$$P_2 = \frac{\gamma_m}{g}(u_2\, c_{u2} - u_1\, c_{u1}) + P_1 - P_V \,.. \quad .. \quad (3)$$

The delivery pressure can, therefore, be affected :

(1) By varying u, by changing the speed.
(2) By varying P_1, for instance, by throttling the suction and thus at the same time reducing γ_m.
(3) By varying P_V, for instance, by adjusting the diffusor section to the momentary volume by means of movable diffusors.
(4) By varying c_{u1}, for instance, by giving the air a certain amount of rotation before entering the impellor, i.e., by pre-rotation.

These four methods of regulation can be divided into two fundamental groups.

I. Regulation by speed variation (1).
II. Regulation at constant speed (2–4).

In the first case the regulation does not take place on the air side, i.e., not in the compressor itself, but in the driving machine.

I. REGULATION BY SPEED VARIATION.

(A) *Variable-speed Motors.*

The following considerations show that it is not an easy matter to obtain with simple means an economical regulation of the speed with motor drive.

(a) The *direct-current motor*, it is true, allows an economical regulation of the speed to be obtained with simple means over a very wide range. Unfortunately it is only in the rarest cases that direct current energy is available in sufficient quantity to supply the high power requirements here concerned, amounting usually to several thousand kilowatts. It would therefore be necessary to install an expensive converter set which would introduce additional losses. Moreover, the speeds of direct-current motors decrease with increasing output. A 1000 kW. motor can be built for a speed of about 1000 r.p.m., but the maximum speed of a 4000 kW. motor could not be much more than about 350 r.p.m. The reduced speed causes, however, not only the cost of the motor, but also that of the gear to increase. The latter cannot be avoided, as the most favourable speed for the compressor lies considerably higher than that for which the motor can be built.

(b) The *three-phase commutator motor*, like the direct-current motor, allows the speed to be varied continuously and economically over a wide range. This type of motor does not, however, come into consideration for driving large steelworks blowers, as it has not so far been possible to build it for the powers here concerned.

(c) The speed of an *induction motor* can be varied in a very simple manner by connecting resistances into the rotor circuit. This method of regulation is, however, as shown by the following argument, associated with losses.

Let

L_G = Power absorbed by the blower = motor power, kW.
L_S = Electrical power transferred from the stator to the rotor, kW.
L_V = Ohmic losses in the rotor circuit kW.
n_0 = Synchronous speed of the motor, r.p.m.
n = Effective motor speed, r.p.m.
c = Speed ratio $= \frac{n}{n_0}$.
s = Slip $= 1 - c$.
L_{G0} = Power absorbed by the compressor at maximum speed ($s = 0$ or $c = 1$), kW.

Because of the smallness of their effect and for the sake of simplicity let the losses in the rotor (apart from the ohmic losses in the rotor circuit) be neglected. Then

$$L_S = L_G + L_V \quad .. \quad .. \quad .. \quad (4)$$

$$L_V = s \,.\, L_S = (1 - c)\, L_S \quad .. \quad .. \quad (5)$$

In the case of a centrifugal compressor the power absorbed varies approximately proportionally to the cube of the speed if, as in the present case, the operating point in the pressure volume diagram moves along a parabola. Hence :

$$L_G = c^3 \,.\, L_{G0} \quad .. \quad .. \quad .. \quad (6)$$

From equations (4), (5) and (6) we obtain :

$$L_V = c^2 \,.\, L_{G0} \,.\, (1 - c) \quad .. \quad .. \quad (7)$$

(Fig. 1). Differentiating with respect to c shows that L_V is a maximum for $c = \frac{2}{3}$ so that :

$$L_{V\max} = \frac{4}{27} L_{G0} \backsim 0.15\, L_{G0} \quad .. \quad .. \quad (8)$$

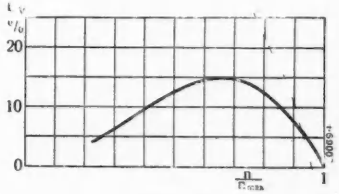

Fig. 1. **Energy which has to be absorbed and converted into useless heat by the resistance during speed variation of a blower driven by an asynchronous motor.**

The rotor resistance must therefore be capable of absorbing continuously a load equal to 15 per cent of the max. compressor power. This requires the provision of a large and expensive water resistance with cooling arrangement and with corresponding electrode wear.

(d) The most economical system of regulation for an induction motor is obtained with the *Brown Boveri Scherbius machine*. Its main characteristic is that it enables the energy which would be otherwise wasted as heat in the regulating resistance of the rotor circuit, to be absorbed by the Scherbius machine and to be converted into useful power. This set enables not only the speed to be regulated both above and below synchronism, but also the power factor to be considerably im-

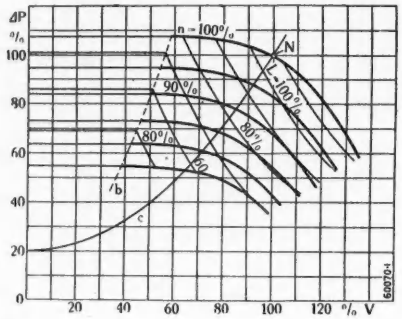

Fig. 2. Pressure, volume curve of a steelworks blower with speed variation. Drive by asynchronous motor with variable resistance in rotor circuit.

Abscissæ : Percentage suction volume.
Ordinates : Percentage rise in pressure.
N. Normal point = 100 per cent point.
n. P–V curves at different speeds in per cent of the normal speed.
b. Pumping limit.
c. Resistance characteristic of the converter.
L. Lines of constant percentage output.

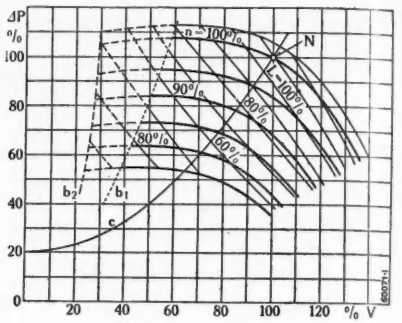

Fig. 3. Pressure volume curves with speed regulation of steelworks blower driven by an asynchronous motor with Brown Boveri Scherbius regulating set.

Abscissæ : Percentage suction volume.
Ordinates : Percentage pressure rise.
N. Normal point = 100 per cent.
n. P–V curves at different speeds in per cent of the normal speed.
b_1. Pumping limit with fixed diffusors.
b_2. Pumping limit with ¾ movable and ¼ fixed diffusors.
c. Resistance characteristic of the converter.
L. Lines of constant percentage terminal load.

proved. The lower limit of the speed is usually about 50 per cent of the maximum. By means of special measures it can be reduced down to 0, which, however, is not necessary in the case of steelworks blowers. The size of the Scherbius machine and therefore its cost increase with the range of speed regulation. For this reason the latter should not be chosen greater than necessary. For steelworks a regulation range of ± 15 to 20 per cent is usually sufficient.

(B) *Behaviour of the Centrifugal Compressor with Change in Speed (Figs. 2 and 3).*

How now, does the blower behave when its speed is changed by means of the driving machine ? Usually, it is designed for entry of the air into the impellers in a radial direction, without rotation, so that $c_{u1} = 0$. Fig. 7 shows the velocity triangle at the entry of the impeller for an inlet angle a. If the speed, and, therefore, u, is varied, then c_1, i.e.—the delivery quantity also must be varied proportionally if the relative direction w is to remain the same and losses are to be avoided. If, however, c_1 changes, then, neglecting the influence of compressibility, the radial component c_{r_2} in the outlet velocity triangle changes in the same ratio ; the outlet velocity diagrams remain similar ; c_{u_2} varies proportionally to u_2, and hence the final result is that the end pressure P_2 must vary as the square of the speed. In other words, the efficiency of the blower remains approximately constant if the end pressure varies proportionally to the square of the volume, that is, when it follows a parabola.

As, however, the resistance of the converter also follows a square law, the change in efficiency of the blower within the operating range is only small. Regulation by speed variation is, for this reason, particularly suitable for converter blowers.

II. REGULATION WITH CONSTANT SPEED.

(A) *The Driving Motor.*

On the basis of our many years of experience, we recommend for large outputs and for high speeds, the synchronous type of motor, which offers considerable advantages. Our rotors are normally built of solid iron without the use of laminations. The rotor winding of synchronous motors is, especially in the case of salient pole machines, very simple. These characteristics, together with the large air gap resulting from the solid rotor, assure an extremely robust design of the rotor. Not only is the efficiency of synchronous motors high, but at a small extra cost they can be made to deliver leading current by increasing the excitation, and thus raise the power factor of the network. These motors are started in a simple manner by means of transformer type starters. If desired, the starting current may be made not to exceed the full load current.

(B) *Possible Methods of Regulation of the Blower at Constant Speed.*

What are the other possible means of regulation when a constant speed motor has been decided upon ? The adaptation of the pressure and air quantity must, in this case, be effected in the blower.

(a) The oldest method of regulation suitable for this purpose is the suction throttling regulation, which due to its simplicity is still frequently used today.

In a blower without cooling, compression of the air takes place along a polytrope according to the law $P \cdot V^n$ = constant, because the unavoidable losses in the blower cause additional heating of the air during compression. The work of compression is then given by :

$$L = G \cdot R \cdot T \frac{n}{n-1}\left[\left(\frac{P_2}{P_1}\right)^{\frac{n-1}{n}} - 1\right]\frac{1}{\eta}\ \frac{\text{m kg.}}{\text{sec.}} \qquad (9)$$

but

$$L = G \cdot H \frac{1}{\eta}\ \frac{\text{m kg.}}{\text{sec.}} \quad .. \quad .. \quad (10)$$

therefore

$$H = R \cdot T \frac{n}{n-1}\left[\left(\frac{P_2}{P_1}\right)^{\frac{n-1}{n}} - 1\right] \text{m} \quad .. \quad (11)$$

The suction throttling does not have any effect either on u or on c_u in equation (1) and hence the delivery head H also remains constant for any given point of the P–V curve. Since the gas constant R in equation (11) also does not change and the variation in inlet temperature T is negligibly small, and finally n remains unaffected because of the constancy of the efficiency, the pressure ratio must remain constant. It follows, therefore, that the end pressure of the blower varies proportionally to the absolute suction pressure.

The weight of air drawn in, and hence also the volume of air V, referred to atmospheric pressure, likewise decreases proportionally to the absolute suction pressure, since the suction volume referred to the pressure P_1 must remain constant when, as remarked above, c_u does not change when u is constant.

If we write equation (9) in the form :

$$L = P_1 V_1 \frac{n}{n-1}\left[\left(\frac{P_2}{P_1}\right)^{\frac{n-1}{1}} - 1\right]\frac{1}{\eta}\ \frac{\text{m kg.}}{\text{sec.}} \qquad (12)$$

it will be seen that the power taken by the blower with suction throttling control, is proportional to the suction pressure P_1, since for a particular point on the P–V curve the remainder of the equation remains unchanged. These conditions are shown graphically in Fig. 4. For a suction pressure less than P_0, the point N wanders along the line d, for instance, down to the point F; for both the end pressure and V vary proportionally to the absolute suction pressure. Since moreover $\frac{P'_2}{P_0} = \frac{P_2}{P_1}$, the suction pressure P_1 lies on the line e at the point G. As can be seen, the line d of maximum blower efficiency follows very closely the resistance characteristic of the converter between the points N and F. In spite of this favourable circumstance, the suction regulation is—as will be seen later—associated with considerable losses.

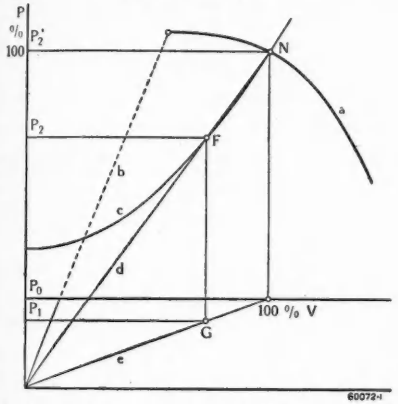

Fig. 4. **Graphical representation of the behaviour of a blower with suction throttling regulation at constant speed.**
With suction throttling it is possible to obtain in a simple manner any operating condition below the unthrottled P–V curve a.
Abscissæ: Percentage suction volume referred to atmospheric pressure P_0.
Ordinates: Right-hand scale = abs. pressure.
Left-hand scale = percentage rise in pressure (for comparison).
P_0. Atmospheric pressure.
P_1. Abs. suction pressure with suction throttling.
P'_2. Abs. end pressure for the normal point N without suction throttling.
P_2. Abs. end pressure for the point F.
a. P–V curve without suction throttling.
b. Pumping limit with suction throttling.
c. Resistance characteristic of converter.
d. Line of constant blower efficiency with suction throttling.
e. Line of absolute suction pressure for end pressures corresponding to line 4.
N. Normal point.
F. Operating point with suction throttling.

Let us assume that the blower is working at the point F of Fig. 4. The effective pressure ratio is $\frac{P_2}{P_1}$, the required ratio is, however, $\frac{P_2}{P_0}$. If L and L_0 are the powers taken corresponding to these two pressure conditions, then the ratio $\frac{L_0}{L}$ may be looked upon as the efficiency of the suction throttling.

$$\eta_s = \frac{\left(\frac{P_2}{P_0}\right)^{\frac{n-1}{n}} - 1}{\left(\frac{P_2}{P_1}\right)^{\frac{n-1}{n}} - 1} \quad .. \quad .. \quad (13)$$

The losses $1-\eta_s$ are shown graphically in Fig. 5. From this diagram it will be seen that for instance, for the point F in Fig. 4 with a specific end pressure of $\Delta P = 65$ per cent, the required pressure ratio is $\frac{P_2}{P_0} = 2.8$, whereas the real pressure ratio is $\frac{P_2}{P_1} = 3.6$ thus giving a throttling loss of $1-\eta_s = 23$ per cent.

(b) *Regulation by means of Movable Diffusors.* A reduction of the losses connected with suction throttling is obtained by the movable diffusor method of regulation introduced by our firm. Its main advantage, however, lies in the fact that the range of stable operation of the blower can be considerably increased. The greater the number of stages provided with movable diffusors, the greater the displacement of the pumping

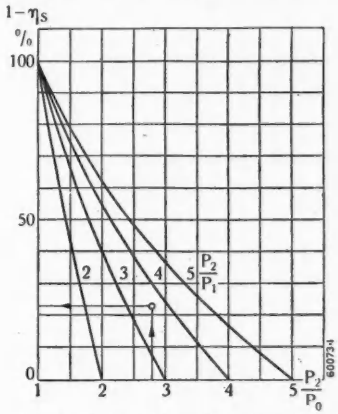

Fig. 5. **Losses with suction throttling.**
The air which has been drawn in at atmospheric pressure P_0 and throttled down to the suction pressure P_1 must again be compressed to atmospheric pressure in the blower with a corresponding waste of power. The diagram shows clearly the way in which the losses increase, when, for instance, with constant $\frac{P_2}{P_1}$ the end pressure and hence $\frac{P_2}{P_0}$ decreases, that is, when in Fig. 7 the operating point F moves along the line d from N down to 0.
Abscissæ: Required pressure ratio $\frac{P_2}{P_0}$.
Ordinates: Percentage power loss due to suction throttling.
Parameter: Effective pressure ratio $\frac{P_2}{P_1}$.

limit in the favourable sense. It is therefore possible to determine the most suitable number of movable diffusors for any given operating conditions.

In order to understand the working of the movable diffusors, it is best to refer back to equation (3). As shown by this equation, the end pressure P_2 may be increased by reducing the losses P_v, other values remaining the same. If a compressor operates with a volume smaller than normal, for instance, in the region of the pumping limit, then the diffusor opening is too large for this reduced volume and the efficiency of the diffusor is correspondingly low*. If, however, the cross-section of the diffusor channel is reduced by moving the blades, in order to adapt it to the smaller volume, its efficiency increases, which with a constant driving power manifests itself as an increase in the

*A. Meldahl: "The Separation of Impellor and Diffusor Losses in Centrifugal Blowers." *The Brown Boveri Review*, August/September, 1941, page 203, & in *The Engineers' Digest*, May, 1942, pp. 172-176.

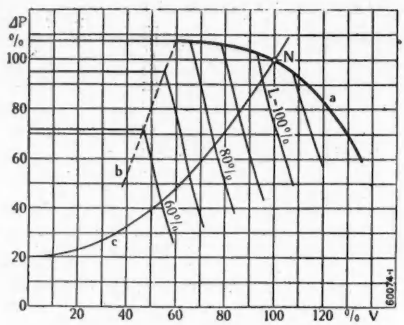

Fig. 6. Pressure-volume curve and power consumption of a steelworks blower synchronous motor drive and suction throttling regulation.
Abscissæ : Percentage suction volume.
Ordinates : Percentage pressure rise.
a. P–V curve without suction throttling.
b. Pumping limit with suction throttling.
c. Resistance characteristic of the converter.
L. Lines of constant percentage terminal power.

end pressure. The maximum pressure of the P–V curve with this smaller diffusor section then lies at a volume lower than the pumping limit volume for the large opening of the diffusor channel; the pumping limit is displaced to the left.

In Fig. 3 the P–V and power curves for the increased range of stable operation to the left of the normal pumping limit obtained with movable diffusors have been drawn dotted. There is a large number of turbo-compressors in service with this form of regulation. It is economical, and from the regulation point of view superior to the suction regulation and to the method of preventing pumping by means of a blow-off valve.

When applied to steelworks blowers, movable diffusors are particularly suitable, if the same converter blower is to be used for blowing widely different charges, under which conditions the resistance characteristic may be very much steeper than normal and may even lie far to the left of the natural pumping limit.

(*c*) *Regulation by Means of Pre-rotation.* If the air enters the blower wheel not radially, but with a certain amount of rotation, then the second member in equation (1) is no longer zero, but assumes either a positive or a negative value depending on the intensity and direction of the rotation. This provides a means for influencing the delivery height *H*.

Figs. 7 D and E show, for instance, the velocity triangles at the wheel inlet and outlet. If we put

$$\frac{r_1}{r_2} = \epsilon \text{ and } \frac{c_{r1}}{c_{r2}} = \nu,$$

and introduce these values with the relations of the velocity triangles in equation (1), then we obtain, upon neglecting the compressibility,

$$H = \frac{u_2^2}{g}\left[1 - \frac{c_{r2}}{u_2}\left(\epsilon \cdot \nu \frac{1}{\tan\delta} + \frac{1}{\tan\beta}\right)\right] \qquad (14)$$

The angle δ is a measure of the rotation with which the air is introduced into the wheel. If $\delta < 90$ deg., then we call it pre-rotation, if $\delta > 90$ deg., then we call it counter-rotation. The values β, ϵ and ν depend on the design of the wheel and for any given wheel they are constant. Equation (14) shows that with constant c_{r2}, that is with constant delivery quantity and constant speed, the delivery height H depends on δ only. If the pre-rotation is increased by reducing δ, then H, and hence the blower end-pressure also decreases.

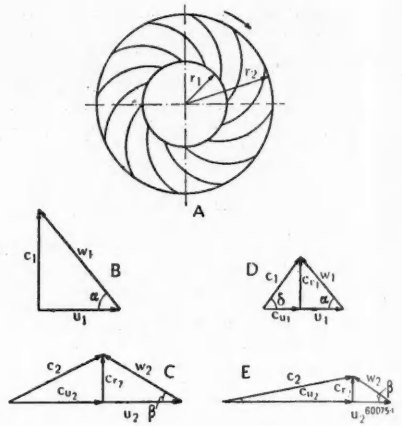

Fig. 7. Velocity triangles at the inlet and outlet of an impeller wheel.
B and C for axial entry without rotation, D and E with pre-rotation (with inlet angle δ).
Pre-rotation causes a variation of cu_1 and cu_2, which according to equation (1) affects the delivery height H of the compressor.
c. Abs. inlet velocity of the air.
c_r. Radial component of the air velocity *c*.
w. Relative velocity.
u. Peripheral velocity.
The indices 1 and 2 refer to the inlet and outlet.

When the end-pressure moves along the resistance characteristic of the converter, a reduction in pressure results also in a reduction of the delivery quantity and hence of c_{r1} and c_{r2}. The velocity triangles at the inlet and the outlet change, result in an alteration of the angle of attack of the blades and hence of the efficiency. By suitably choosing the values a, β, ϵ, ν, it is possible to design the blower so that the incidence conditions of the blades remain as favourable as possible when the pressure and delivery quantity vary according to the resistance characteristic of the converter. (See Fig. 8).

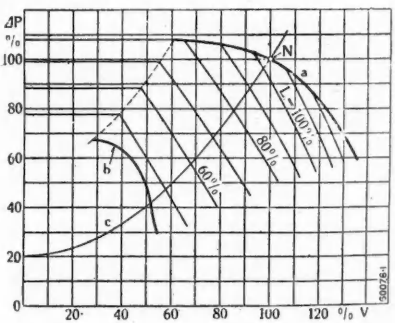

Fig. 8. Pressure-volume curves with regulation by pre-rotation. Drive by means of a synchronous motor.
The normal range of regulation for various positions of the guide blades lies between the P–V curves a and b.
Abscissæ : Percentage suction volume.
Ordinates : Percentage pressure rise.
a. P–V curve without pre-rotation.
b. P–V curve with pre-rotation.
N. Normal point.
c. Resistance characteristic of the converter.
L. Lines of constant percentage terminal output.

Fig. 9. **Example of a Brown Boveri pre-rotation ring containing the movable blades, which give the required rotary movement to the air by a corresponding adjustment of the position of the blades.**

The guide blades can be adjusted during operation from the outside, enabling regulation of the delivery quantity at constant speed of the compressor.

(d) *Comparison of the Power taken by the different Forms of Regulation described.* The relative merits of the various forms of regulation can be seen from Fig. 10. This figure shows the power taken at the motor terminals as a function of the suction volume, for the case that the pressure and volume vary according to the converter characteristic referred to at the beginning of this article. The curves have been obtained from Figs. 2, 3, 6 and 8.

This diagram can be used to compare the energy required for blowing a charge in a particular case. With the aid of Figs. 2, 3, 6 and 8 it is possible to determine the relative average power consumption for every type of regulation. Taking that required for suction regulation as equal to 100, we have :

(a) Suction regulation	100 per cent
(b) Resistance regulation ..	95.1 per cent
(c) Pre-rotation	92.8 per cent
(d) Scherbius regulation ..	90.7 per cent

The energy consumption with the four systems of regulation for blowing a single charge with a blower rating of for instance 3500 kW. would be as follows :—

(a) 829 kWh.
(b) 788 kWh.
(c) 769 kWh.
(d) 752 kWh.

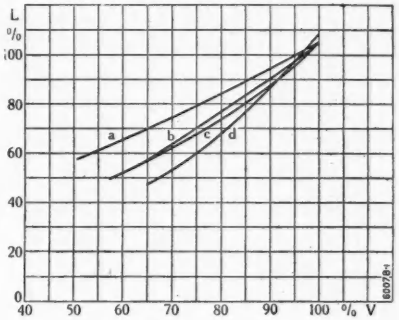

Fig. 10. **Comparison of the power consumption of different methods of regulation.**

The comparison is based on the same resistance characteristic and the same coupling of the blower at the normal operating point. The curves show the increasing economy of the different methods of regulation in the order a—d, the power consumption for a volume of for instance 80 per cent decreasing from 84.5 to 67.5 per cent.
Abscissæ : Percentage suction volume.
Ordinates : Percentage motor terminal power
a. Suction throttling with synchronous motor drive.
b. Speed regulation by induction motor with resistance in the rotor circuit.
c. Regulation by means of pre-rotation with synchronous motor drive.
d. Speed regulation by means of induction motor with Scherbius regulating set.

This example shows that, for a given blowing diagram, it is possible in every case to determine the most favourable system of regulation of the converter blower after taking into account the cost of power, and the operating and capital charges. The operating conditions in different plants may differ appreciably. For this reason, the figures given above must be considered as providing an indication only, and it is advisable, if only because of the rapid progress being made, for a close contact to be maintained between steelworks and blower engineers.

In this connection it is worth mentioning that it is advantageous not to choose the blower larger than is necessary, in order that the operating range shall really lie in the region of maximum efficiency and thereby avoid, especially in the case of blowers with fixed diffusors, that the blow-off valve shall operate frequently, a process which is always associated with losses. All methods of regulation can be arranged for remote control, so that they can be operated from the converter stand.

NOVEL PHOTOELECTRIC PYROMETER.

By E. VIRASORO and G. BERRAZ. (From *Revista Electrotecnica*, Buenos Aires, Vol. 31, February, 1945, pp. 56-60).

THE employment of photoelectric cells for the measurement of high temperatures has been repeatedly suggested. B. M. Larsen and W. E. Shenk* studied the action of a pyrometer equipped with a selenium cell, the photocurrent of which is a function of the radiant block body temperature. Selenium photocells react to wave lengths between 4000 and 8000 Ångstrom, their maximum sensitivity approximating to a wave length of 6000 Å. Up to 1000 deg. C., the emission of energy by an incandescent solid body takes place almost exclusively by infra-red radiation, that is, a range of waves to which the selenium cell is not responsive. With higher temperatures, however, the energy emission by luminous radiation increases rapidly, causing a photoelectric effect which can be made to serve as a measure of the temperature of the emitting body, by calibrating the instrument by means of an optical pyrometer.

A pyrometer with two vacuum cells of the Cs–O–Ag type equipped with green and red filters was developed by H. W. Russel, C. F. Lucks, and L. G. Turnbull. In this instrument the respective responses of the two cells, exposed to a common source of light are dependent upon the respective radiations passed by the filters. With an increase in temperature the amount of radiant energy passed by the green filter increases as compared to that passed by the red filter, and a correction is therefore required. Although calibration with the employment of an optical pyrometer is required, this photoelectric instrument possesses the advantage of permitting the direct recording of temperatures within a range from 1,000 to 2,000 deg. C.

*Temperature : its Measurement and Control in Science and Industry, 1941, p. 1150.

When comparing the spectral sensitivity of selenium and of thallous sulphide cells the idea presented itself to adapt these cells to the measurement of the temperature of incandescent solid bodies.

Two barrier layer cells, one of the selenium and the other of the thallous sulphide variety, may be arranged side by side in such a manner that they intercept equivalent fluxes of radiation emitted by an incandescent solid body. The two cells may be connected to galvanometers or to micro-ammeters of low resistance. The photocurrent produced by each of the cells will be proportional to the intensity of the incident radiation. If the position of the radiant source is changed, the intensities of the individual cell currents i_{Se} and i_{STl_2} will vary in inverse proportion with the square of the distance and with the cosine of the angle of incidence, but the ratio $\frac{i_{Se}}{s_{STl_2}}$ will remain unaltered, provided the spectral distribution of the radiant energy remains unchanged.

If the temperature of the radiant solid body increases, the total energy irradiated will increase with the fourth power of the absolute temperature T (Stefan's law) and at the same time the spectral distribution will change, the maximum of the distribution curve being displaced into regions of shorter wave lengths. This displacement will be reflected by a corresponding increment of the photocurrents i_1 of the selenium cell and i_2 of the thallous sulphide cell. This increment will be relatively greater in the case of the selenium cell, which is to say that the ratio $\frac{i_1}{i_2}$ will increase with the temperature of the incandescent body. This fact is illustrated in Fig. 1, where the curves S and T represent the spectral sensitivities of the selenium cell and of the thallous sulphide cell respectively, the ordinate showing percentages of maximum sensitivity and the abcissa giving the wave length μ. Curves A, B, C, and D represent the spectral energy distributions of the black body at different temperatures in degrees Kelvin. Maximum sensitivity of the selenium cell is seen to occur at a wave length of 0.6 μ, and that of the thallous sulphide cell at 0.94 μ.

In Fig. 2 it is shown how a combined selenium and thallous sulphide cell arrangement can be utilised for the purpose of temperature measurement. Here a 500 Watt lamp L with tungsten coil is connected to a supply circuit comprising a variable transformer Tr, a rheostat R, and a voltmeter V. The filament temperatures corresponding with the different voltages prevailing at the lamp terminals are measured by means of the optical pyrometer P.O. of the Fisher & Foote type. This pyrometer is focussed upon the lower portion of the lamp filament.

The photocurrents i_1 and i_2 originating in the photocells T and S were measured at various filament temperatures. In order to avoid faulty indication because of a gradual heating of the cells by radiation, the latter were shielded by a screen which was only removed during the time of actual temperature measurement. The test results recorded are listed in Table I., which extends to an upper temperature limit of 1795 deg. C.

TABLE I. THALLOUS SULPHIDE.

Voltage v	Temp°e	i_1 (Se) μ A	i_2 (STl_2) μ A	$\frac{i_1}{i_2}$
35	1070	0.7	15.9	4.4×10^{-2}
40	1148	1.4	27.5	5.1
45	1194	2.9	43.5	6.7
50	1261	5.0	62.0	8.1
55	1317	8.5	84.0	10.1
60	1360	13.0	110.0	11.8
65	1394	20.1	150.2	13.4
70	1462	29.8	173.9	17.1
75	1513	40.0	208.0	19.2
80	1555	52.0	243.0	21.4
85	1590	68.0	285.3	23.8
90	1621	87.5	341.8	25.6
95	1655	110.0	386.4	28.5
100	1700	133.7	427.2	31.3
105	1730	167.2	480.7	34.8
110	1750	200.6	533.5	37.6
115	1760	237.8	588.5	40.4
120	1795	277.9	635.3	43.7

This temperature limit, however, was solely due to certain experimental difficulties not connected with the operating principle of the apparatus as such. A graphic representation of these test results is given in Fig. 3. The actual accuracy of this experimental instrument has not been determined, but from the shape of the curve, it can be deduced that accuracy of measurement increases with the temperature, at least within the range of the experiment.

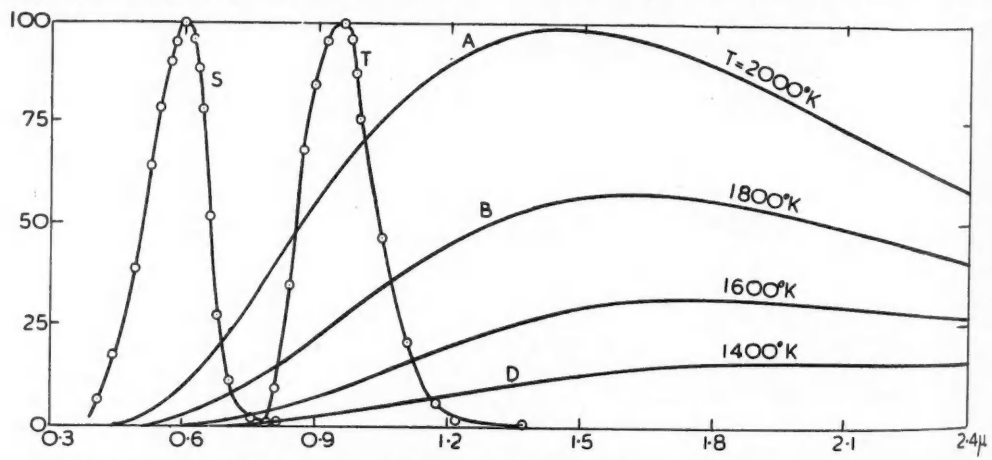

Fig. 1. Spectral sensitivities of selenium and thallous sulphide cells.

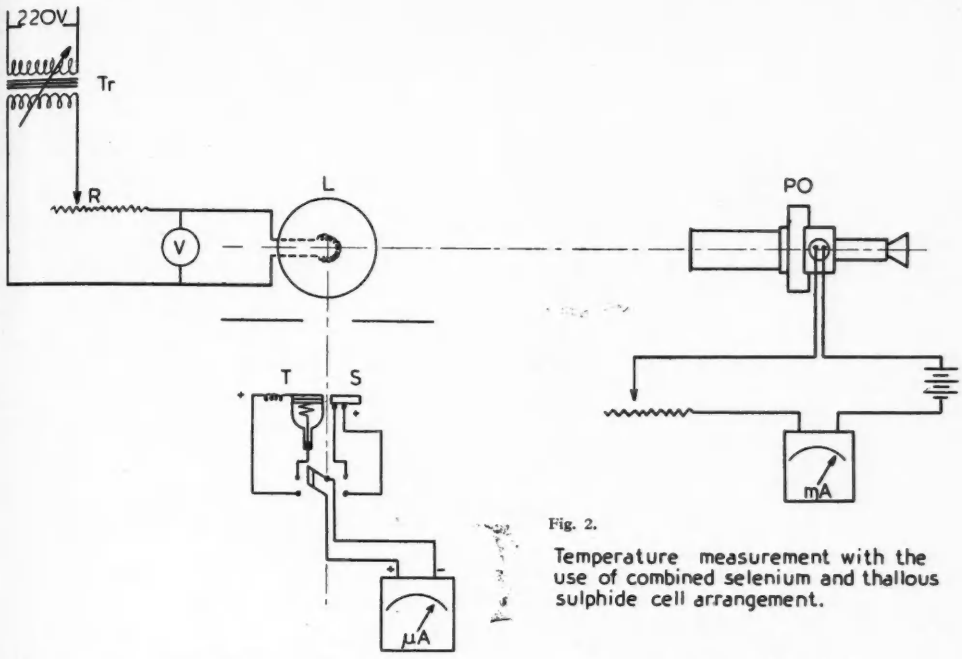

Fig. 2.

Temperature measurement with the use of combined selenium and thallous sulphide cell arrangement.

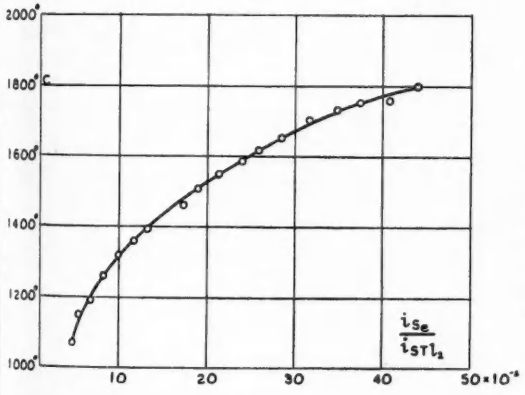

Fig. 3. Ratio of cell currents

An approximate analytical expression relating temperature and cell currents can be established on the basis of Wien's law. According to the latter, the energy $E(\lambda_1 T)$ emitted by a black body of the absolute temperature T (corresponding to a wave length λ) is given by the expression

$$E(\lambda_1 T) = \alpha \lambda^{-5} e^{B/\lambda T}$$

where α and β are constants. For two monochromatic radiations λ_1 and λ_2 the corresponding energies emitted by the black body at the temperature T are $E_1 = \alpha . \lambda_1^{-5} e^{B/\lambda_1 T}$ and $E_2 = \alpha . \lambda_2^{-5} e^{B/\lambda_2 T}$

By dividing E_1 by E_2, we have

$$\frac{E_1}{E_2} = \left(\frac{\lambda_2}{\lambda_1}\right)^5 e^{B/TC\lambda_1 - \lambda_2}$$

On the logarithmic basis it is therefore

$$\ln \frac{E_1}{E_2} = 5 \ln \frac{\lambda_2}{\lambda_1} + \frac{\beta(\lambda_1 - \lambda_2)}{T}$$

This expression can be simplified to read

$$\log_{10} \frac{E_1}{E_2} = A + \frac{B}{T} \quad .. \quad .. \quad .. \quad (1)$$

Actually the validity of this expression is limited to the case of monochromatic radiation of the wave lengths λ_1 and λ_2, but in first approximation it can be extended to the case of two distinct regions of the same spectrum. In the case under consideration these regions will cover a range of 4,000–8,000 Å. applying to the selenium cell and of 8,000–12,000 Å. applying to the thallous sulphide cell. If it is assumed that the photo-currents i_1 and i_2 of the cells are proportional with the incident energies, $\frac{E_1}{E_2}$ can be replaced by $\frac{i_1}{i_2}$, and equation (1) therefore takes the form $\log_{10} \frac{i_1}{i_2} = A + \frac{B}{T}$

By further making $y = \log_{10} \frac{i_1}{i_2}$ and $x = \frac{1}{T}$, this expression becomes a linear function of the type $y = A + Bx$. The admissibility of this assumption is confirmed by the graph shown in Fig. 4, this graph being based upon the values for $\frac{1}{T}$ and $\log. \frac{i_1}{i_2} \times 10^2$ given in Table II.

Equation (1) may also prove useful in the calibration of pyrometers of this type, as it permits establishment of the calibration curve by simply drawing a straight line through two established points.

The design of a pyrometer of this type for use in practice is visualised as follows: The selenium and the

TABLE II.

T	$\frac{1}{T}$	$\frac{i_1}{i_2}$	$\log \frac{i_1}{i_2} \times 10^2$
1343	74.5×10^{-5}	4.4×10^{-2}	0.64345
1421	70.4	5.1	0.70757
1467	68.2	6.7	0.82607
1534	65.2	8.1	0.90849
1590	62.9	10.1	1.00432
1633	61.3	11.8	1.07188
1667	60.0	13.4	1.12710
1735	57.6	17.1	1.23300
1786	56.0	19.2	1.28330
1828	54.7	21.4	1.33041
1863	53.7	23.8	1.37658
1894	52.8	25.6	1.40824
1928	51.9	28.5	1.45484
1973	50.7	31.3	1.49554
2003	49.9	34.8	1.54158
2023	49.4	37.6	1.57519
2068	48.4	43.7	1.64048

thallous sulphide cells are placed side by side at the bottom end of a blackened tube, the open end of which is to be focussed upon the spot the temperature of which is to be measured. The thallous sulphide cell is to be provided with an iris diaphragm externally adjustable by means of a dial.

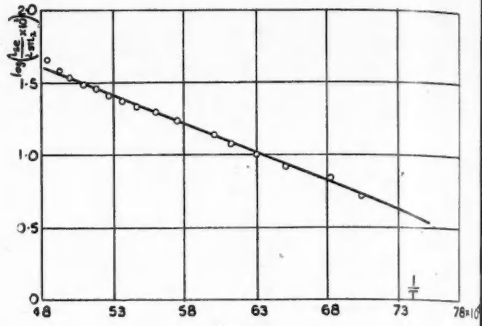

Fig. 4.

This instrument will have to be furnished with a differential galvanometer equipped with a moving coil system carrying two windings, the latter two being connected to the two cells in such a manner that the cell currents oppose each other. Measurement is carried out by modifying the intensity of the radiation incident upon the thallous sulphide cell by adjusting the iris diaphragm until the galvanometer needle has returned into the zero position. The dial of the iris diaphragm may be directly graduated in degrees of temperature.

TEMPERATURE DISTRIBUTION AND HEAT FLOW IN BARS.

By H. BLOM-ANDERSEN. (From *Ingenioren*, No. 81, December 9th, 1944, pp. 169-171).

IN this article a " bar " is defined as a body isolated from its surroundings and of constant cross section, and also of such dimensions that in all cross-sectional planes the temperature is uniform throughout. By choosing a cross-sectional datum plane, the temperature and the heat flow prevailing at an arbitrarily chosen second section may be expressed by a function of the distance X between the two planes. Thus, if the possibility of heat transfer along the surface of the bar is excluded, the lengthwise heat flow in the bar can be expressed by

$$V_A = F \cdot \lambda \cdot \frac{\Delta t}{\Delta x}$$

where F is the cross-sectional area of the bar, λ is the thermal conductivity of the material, and Δx and Δt are defined as indicated in Fig. 1. By decreasing the distance Δx between the two planes the equation for V_A will finally assume the form

$$V_A = F \cdot \lambda \cdot \frac{dt}{dx}. \qquad (1)$$

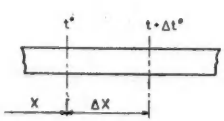

Fig. 1.

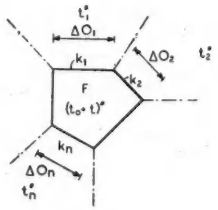

Fig. 2.

In this expression the heat flow is taken to have the positive sign if the temperature increases with the distance X. Referring to Fig. 1, if a heat flow V_A passes through the section corresponding to the temperature t^0, the amount of heat lost through the surface over the distance Δx will be ΔV_A and the loss per unit length will be

$$V_B = \frac{\Delta V_A}{\Delta X} \text{ or } V_B = \frac{dV_A}{dX}.$$

By introducing expression (1) it becomes

$$V_B = \frac{d\left(F \cdot X \cdot \frac{dt}{dx}\right)}{dx} = F \cdot \lambda \frac{d^2t}{dx^2} \quad .. \quad (2)$$

For the case of a uniform circumambient temperature t_0, it is $V_B = K \cdot O \cdot t$, where K is the coefficient of heat transfer from the surface of the bar to the surrounding medium, O is the circumference of the bar and t is the difference between the temperature of the surface of the bar and the surrounding medium. Equation (2) can therefore be written

$$\frac{d^2t}{dX^2} = \frac{O \cdot K}{F \cdot \lambda} \cdot t$$

In the general case, shown in Fig. 2, the circumference of the bar is assumed to consist of a number of individual strips ΔO_1, ΔO_2, etc., each having its own particular heat transfer coefficient K_1, K_2, etc., and being exposed to a different ambient temperature t_1, t_2, etc. The equilibrium temperature of the bar may be denoted by t_0. This will obtain when heat supply and heat loss take place solely through the surface of the bar.

The heat loss suffered by the bar is represented by the sum total of the individual losses and as such will be given by

$$V_B = \Sigma k_n \cdot \Delta o_n (t + t_0 \div t_n) = t\,\Sigma k_n \cdot \Delta o_n + \Sigma k_n \Delta o_n \quad .. \quad .. \quad (3)$$
$$(t_0 \div t_n)$$

In the state of equilibrium ($t = O$), it would be $V_B = O$, and it is therefore

$$V_B = t \cdot \Sigma k \cdot \Delta o$$

By introducing this value into expression (2) we obtain

$$\frac{d^2t}{dx^2} = \frac{\Sigma k \cdot \Delta o}{F \cdot \lambda} \cdot t \quad .. \quad .. \quad (4)$$

In this expression the differential quotient is seen to be independent of the dimensions of the bar, of its temperature condition, and of the choice of the datum point. With the introduction of

$$\alpha = \sqrt{\frac{\Sigma k \,.\, \Delta o}{F \,.\, \lambda}}$$

the integral of expression (4) is found as

$$t = A \,.\, e^{\alpha x} + B\, e^{\div \alpha x} \quad .. \quad .. \quad (5)$$

and by combining with expression (1):

$$V_A = \alpha\,(A \,.\, e^{\alpha x} \div B\, e^{\div \alpha x})\, F \,.\, \lambda \quad .. \quad (6)$$

Equations (5) and (6) therefore represent general expressions for the temperature and heat flow distribution respectively in a bar provided that (1) the cross section of the bar is constant over the length of the bar and the ambient temperature is also constant over the entire length of the bar; (2) the heat exchange takes place through the surface of the bar. Furthermore, it should be noted that the temperature t (equation 5) is not the temperature of the bar, but represents the difference between the actual temperature of the bar and the equilibrium temperature t_0, which in turn depends upon the surface insulation of the bar and upon the ambient temperature.

In order to demonstrate the application of expressions (5) and (6), a bar of the length *a* metres, one end of which is heated to the temperature T_0 above the equilibrium temperature t_0, while the other end of the bar is at the equilibrium temperature t_0, will be considered.

At the heated end, which is used as reference point, it will be $X = O$ and $t = T$. By introducing these values into expression (5) it is found: $A + B = T$.

The cold end of the bar is characterised by $X = a$ and $t = O$, and it is therefore $A \,.\, e^{\alpha a} + B\, e^{\div \alpha a} = O$. Solving for A and B, we obtain

$$A = \div \frac{1}{e^{2\alpha a} \div 1} \,.\, T \text{ and } B = + \frac{e^{2\alpha a}}{e^{2\alpha a} \div 1} \,.\, T$$

The actual values for A and B will naturally depend upon the length of the bar and its other dimensions; but it is seen that their influence upon the temperature distribution only depends upon the products $\alpha \,.\, a$; and in the case of bars of identical cross section, the product $\alpha \,.\, a$ is a measure of the length of the rod.

In Fig. 3 are given a number of curves which show the temperature margin t prevailing with different values for $\alpha \,.\, a$, while the subjoined table I. lists corresponding values for A and B. For $\alpha \,.\, a = O$ it is $A = \div \infty$ and $B = \infty$. As will be seen from Fig. 3, in the case of short bars ($\alpha \,.\, a = 1$) the temperature curve approximates to a straight line. This is due to the fact that the main portion of the heat supplied from the heated end of the bar is passed on to the other end of the bar, while only a small amount of heat is dissipated from the surface of the bar. However, as the factor $\alpha \,.\, a$ is increased, more and more heat will be dissipated from the surface of the bar and the corresponding temperature curves will exhibit a correspondingly greater curvature; and, already with a value of $\alpha \,.\, a = 2 - 3$, the temperature curve toward the heated end will approach a shape corresponding to that found with $\alpha \,.\, a = \infty$.

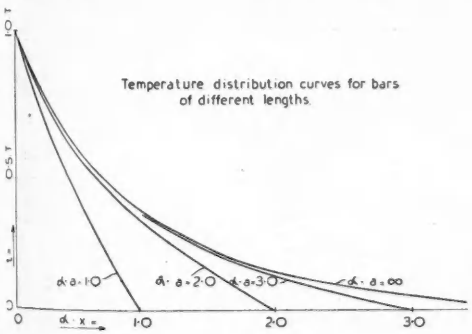

Fig. 3.

By introducing values for A and B into equation (6) the heat flow in the bar can be determined for any point along the length of the bar. Of particular interest is the point in the immediate vicinity of the heated end. At this point, which is characterised by $X = O$ and $e^{\alpha x} = 1$, the heat flow is given by

$$V = \frac{B \div A}{T} \,.\, \alpha \,.\, F \,.\, \lambda \,.\, T = C \,.\, \alpha \,.\, \lambda \,.\, F \,.\, T \quad (7)$$

For $\alpha \,.\, a = O$ it is $C = \infty$; but with increasing values of $\alpha \,.\, a$, C undergoes a rapid decrease, reaching a minimum value of $C = 1$ for $\alpha \,.\, a = \infty$. Excluding very short bars ($a\alpha < 2 - 3$) the factor C, and consequently the heat flow requirements, will practically be independent of the length of the bar.

Heat flow by conduction is generally expressed by

$$V = \frac{\lambda}{z} \,.\, F \,.\, T \quad .. \quad .. \quad (7a)$$

where F is the flow area, λ is the thermal conductivity, z is the length of the flow path and T is the temperature difference existing between the two terminal surfaces. By comparing this expression with equation (7), it is easily seen that in the case under consideration the heat flow in the proximity of the hot end of the bar corresponds to the flow passed through a bar with perfectly insulated surface of the "equivalent length"

$$Z = \frac{1}{C \,.\, \alpha}.$$

TABLE I.

αa	$\frac{A}{T}$	$\frac{B}{T}$	C	$\lambda \div \alpha a$
0.0	$\div\infty$	∞	∞	1.000
0.2	$\div$2.03	3.03	5.06	0.819
0.4	$\div$0.82	1.82	2,64	0.670
0.6	$\div$0.43	1.43	1.86	0.549
0.8	$\div$0.252	1.252	1.50	0.449
1.0	$\div$0.157	1.157	1.31	0.368
1.2	$\div$0.100	1.100	1.20	0.301
1.4	$\div$0.065	1.065	1.13	0.247
1.6	$\div$0.042	1.042	1.084	0.202
1.8	$\div$0.0281	1.028	1.056	0.165
2.0	$\div$0.0187	1.019	1.037	0.135
2.5	$\div$0.0068	1.007	1.014	0.0822
3.0	$\div$0.0025	1.003	1.005	0.0498
3.5	$\div$0.0009	1.001	1.002	0.0302
4.0	$\div$0.0003	1.000	1.001	0.0183
5.0	$\div$0.00005	—	1.000	0.0067
∞	0	1	1	0

PRESSURE LOSSES IN BRANCHES OF SQUARE CHANNELS.

By Dr. Ing. M. A. IBRAHIM and Dipl. Ing. M. A. HASSAN, Giza (Egypt). (From *Schweizerische Bauzeitung*, Vol. 124, No. 4, July, 1944, pp. 48-50).

INTRODUCTION.

WHEN subdividing an air-stream into two branches pressure losses occur; the same is the case when the two branches unite. The magnitude of the pressure loss in a branch is dependent on the angle of deflection of the branch and on the ratio of the mass flows in the two channels. Under certain conditions the pressure loss can amount to more than 90 per cent of the dynamic pressure in the main stream. It is important for the designer to know:

1. The change of pressure loss with variable working conditions, and

2. What aids can be employed to reduce these losses to a minimum.

The present investigation has been undertaken in the Institute for Aerodynamics of the Swiss Federal Technical College, and is due to the encouragement of Prof. Dr. Y. Ackeret.

The range covered was:

1. Determination of pressure losses in branches of 45 deg. and 90 deg.;

2. The influence of installing a rigid flow-guide into the 90 deg.-branch.

THE TEST SET-UP.

Branches of square cross-section have been installed between one inflow channel A and two outflow channels B and C of the same cross-section (Fig. 1). The entry to channel A was through a metering nozzle MD which was connected by a corner to the electrically driven blower (12 h.p.). To eliminate the disturbance caused by the corner, a flow-equalizing grid has been installed in front of the nozzle. All channels were of ply-wood, inside lacquered and carefully polished. All joints have been sealed. The rigid flow-guides were wooden inset pieces, lacquered (detail H in Fig. 1), and so chosen that there was only little break-away at the corners. Measurements have been taken at 28 points (see Fig. 1) by means of micro-manometers, the range of which was 300 mm. water column, and their accuracy 1/10 mm. H_2O.

NOTATION AND DIMENSIONS.

q [kg./m²] $= \rho/_2\, v^2$	= dynamic pressure
ρ [kg./sec² m⁻⁴]	= air density
v [m/sec.] $= Q/F$	= mean air speed over the cross-section.
F [m²]	= cross-sectional area.
L [m]	= channel length.
p [kg./m²]	= static wall pressure
p_{th} [kg./m²]	= theoretic wall pressure without branch loss
p_{tc} [kg./m²] $= p_{th\text{-}c} - \delta_{abg}$	= fictitious wall pressure in channel C
p_{tB} [kg./m²] $= p_{th\text{-}b} - \delta_{ger}$	= fictitious wall pressure in channel B
δ_{abg} [kg./m²]	= branch pressure loss, sections a to c
δ_{ger} [kg./m²]	= pressure loss in straight part, sections a to b
δ_{RA}, δ_{RB} and δ_{RC} [kg./m²]	= friction pressure loss in A, B and C
Δp_{MD} [kg./m²]	= pressure drop in metering nozzle
Δp_{RD} [kg./m²]	= pressure drop in control nozzle
$\zeta_{abg} = \delta_{abg}/q_a$,	= Loss coefficient
$\zeta_{ger} = \delta_{ger}/q_a$,	= Loss coefficient
$R_e = \dfrac{\frac{4F}{U} \cdot v}{\gamma}$	= Reynold's number
U [m]	= perimeter of cross section
ν [m²/sec.]	= kinematic viscosity of air
m	= ratio of cross-sections of channel to nozzle RD
$\alpha = \dfrac{Q_{MD}}{Q_{RD}}$	= calibration number of nozzle
Q [m³/sec.]	= mass flow of air

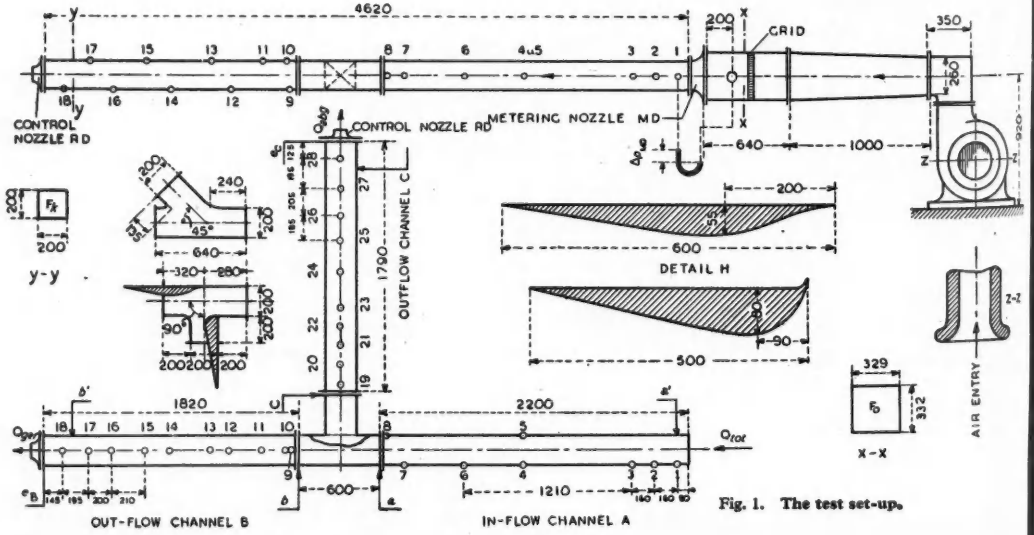

Fig. 1. The test set-up.

Indices : K for measuring channel
O for channel in front of metering nozzle
MD for metering nozzle
RD for control nozzle
abg for branch
ger for straight

THEORY OF BRANCH LOSSES SELECTION OF CROSS-SECTIONS.

The branching of an air-stream is in effect a deflection with varying magnitude over the cross-section of single stream-lines and therefore sections such as a, b and c (Fig. 1) are unsuitable for measuring δ_{abg} and δ_{ger}, as the pressure is not constant over the cross-section. Measurement can be undertaken at some distance from the branch where the flow is more or less parallel. Sections such as a', b' and c' fulfil this requirement but the measured pressure losses include the pressure losses due to friction in the straight channels A, B and C. To separate from the branch losses δ_{abg} and δ_{ger} the losses δ_{RA}, δ_{RB} and δ_{RC}, the latter must be determined by preliminary tests.

In accordance with the ratio m, there is a more or less pronounced curvature of the vortex lines (Fig. 2), which make also sections e_B and e_C at the end of the outflow channels unsuited for taking measurements. Therefore, the chosen sections b' and c' are located at a fixed distance l in front of the control nozzles. Measuring the wall pressures before the sections b' and c' (Fig. 3) one can see whether in these sections the flow recovered from the disturbance due to branching. This is the case when the wall pressure distribution is identical with that due to friction loss at the prevailing Reynolds number.

THE PRINCIPLE OF MEASUREMENT.

Due to branching the speed in channels B and C is smaller than that of the original stream A. Applying Bernoulli's equation to sections a and b, and a and c respectively, the theoretical pressures at these sections will be $p_{th\text{-}b}$ and $p_{th\text{-}c}$, as shown in Fig. 2. These pressures would actually exist if there were no losses δ_{abg} and δ_{ger} due to branching.

Introducing further the following fictitious pressures

$$\left.\begin{aligned} p_{fB} &= p_{b'} + \delta_{RB} \\ p_{fC} &= p_{c'} + \delta_{RC} \end{aligned}\right\} \quad .. \quad .. \quad .. \quad (1)$$

these would prevail at the sections b and c if there was no disturbance due to branching.

It is also

$$\left.\begin{aligned} \delta_{ger} &= p_{th\text{-}b} - p_{fB} \\ \delta_{abg} &= p_{th\text{-}c} - p_{fC} \end{aligned}\right\} \quad .. \quad .. \quad .. \quad (2)$$

If these losses are divided by the dynamic pressure at section a' a very convenient loss coefficient is obtained :

$$\zeta_{ger} = \frac{\delta_{ger}}{q_{a'}} \text{ and } \zeta_{abg} = \frac{\delta_{abg}}{q_{a'}} \quad .. \quad .. \quad (3)$$

The measured wall pressures are shown in Fig. 3, as well as the application of the principle of measurement to a 45 deg. branch. At this measurement 36.7 per cent of the total mass passed through channel C.

THE FRICTION LOSS IN THE STRAIGHT PARTS.

The coefficient of friction λ has been measured and is plotted in Fig. 4 against Reynolds number.

The friction loss δ_R is given by the equation

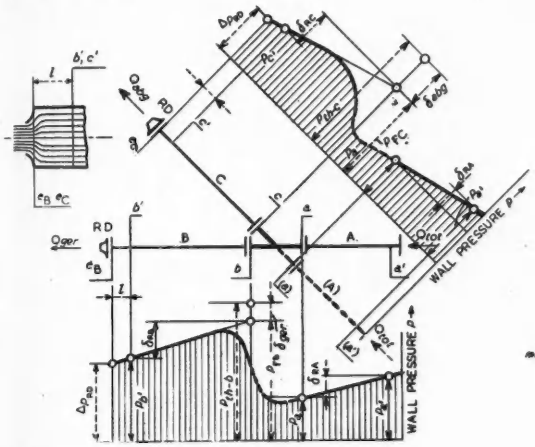

Fig. 2. **Illustrating the principle of measurement.**

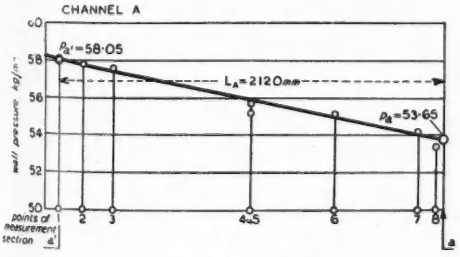

Fig. 3a.

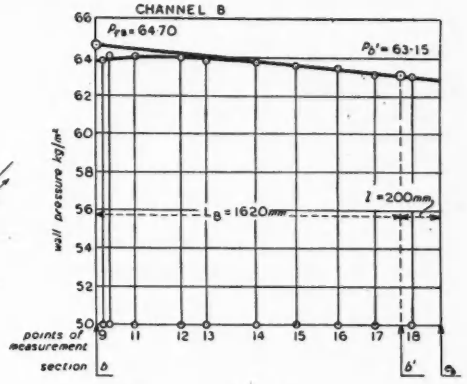

Fig. 3b.

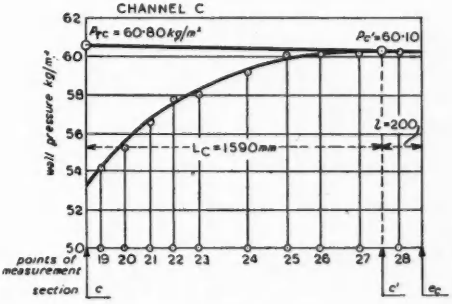

Fig. 3c.

Fig. 3. Measured pressure distribution in the channels A, B and C with 45 deg. branch.

$$\delta_R = \lambda \frac{L}{\frac{4F}{U}} \rho/2\, v^2 \quad .. \quad .. \quad .. \quad (4)$$

MEASUREMENT OF MASS FLOW.

The total mass Q_{tot} has been measured by means of a metering nozzle (Fig. 1). Q_{ger} and Q_{abg} have been also measured as a check on the value obtained from the continuity equation. These mass flows were obtained by using the control nozzles. The nozzles have been calibrated. Two equations are necessary for the calculations :

$$\Delta p_{MD} = q_K \left[1 - \left(\frac{F_K}{F_O}\right)^2\right] \quad .. \quad .. \quad (5)$$

and

$$q_K = \rho/2\, v_K^2 = \frac{\Delta p_{RD}}{(m/\alpha)^2 - 1} \quad .. \quad .. \quad (6)$$

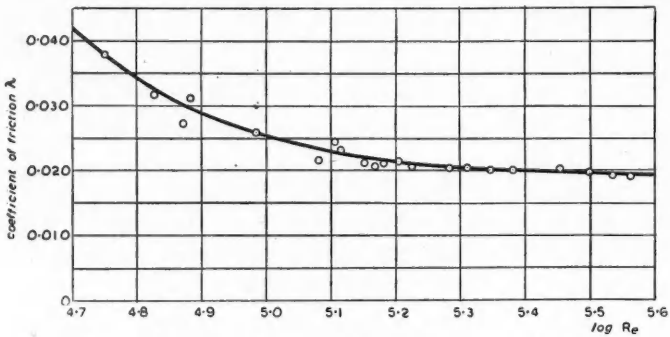

Fig. 4. Co-efficient of friction as a function of Reynolds' number.

From eq. (6) the speed v_K is determined. The α-values found by calibrating, are given in the table below :

Dia. of control nozzle mm.	$m = \frac{0.04}{F_{RD}}$	α	$(m/\alpha)^2 - 1$
130	3.014	1.005	8
100	5.093	1.018	24
50	20.372	1.000	414

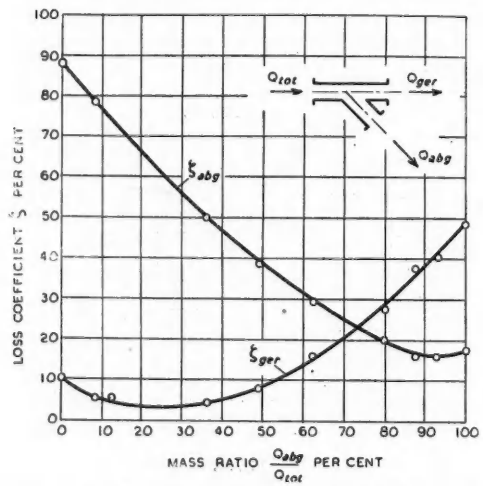

Fig. 5. Loss co-efficient against mass ratio 45 deg. branch.

THE PRINCIPAL TESTS AND RESULTS.

Figs. 5, 6 and 7 show the loss coefficients ζ_{ger} and ζ_{abg} plotted against air mass ratios for the three types of branches investigated. The change of the air mass ratio was obtained by a set of control nozzles. For the mass ratio 0 per cent, one or the other outflow channel was closed. It has been found that the loss coefficient is practically independent of the Reynolds number.

The results of these tests are clear from Figs. 5, 6 and 7. It is evident that the greater deflection of the branch, the higher the loss in the branch. In the straight channel the loss is practically independent of the magnitude of deflection. It is also well shown that by suitable flow guides the losses can be considerably reduced.

EXAMPLE OF APPLICATION.

In the pipes of a ventilating plant, 1500 m. above sea level, the air speed is 10 m./sec. The pipes are of square section, U = 300 mm. The air is branched into two pipes of equal section under 90 deg. so that 60 per cent of Q_{tot} is flowing through the deflected pipe. The outflow channels are each 5 m. long. What are the losses in these and in the branch? According to C.I.A.N. Standard Atmosphere at 1.5 km. height t = 5.25 deg. C; p = 8615 kg./m²; γ = 16.12 × 10⁻⁶ m²/sec., and ρ = 0.1079 kg. sec². m⁻⁴.

In the inflow channel :

$$q = \frac{0.1079 \times 10^2}{2} = 5.395 \text{ kg./m}^2$$

$$R_e = \frac{4 \times 0.3^2 \times 10}{4 \times 0.3 \times 16.12} \times 10^6 = 0.185 \times 10^6$$

Determination of branch losses :

For branching of 60 per cent. of the mass flow according to Fig. 6.

ζ_{abg} = 74 per cent, thus $\delta_{abg} = 0.74 \times 5.395 = 4$ kg./m²

ζ_{ger} = 14.8 per cent, thus $\delta_{ger} = 0.148 \times 5.395 = 0.796$ kg./m².

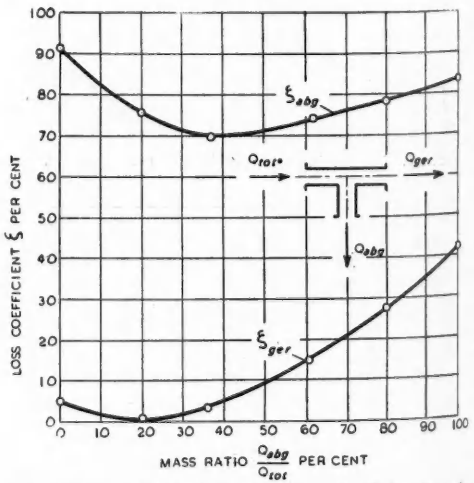

Fig. 6. Loss coefficient against mass ratio 90 deg. branch.

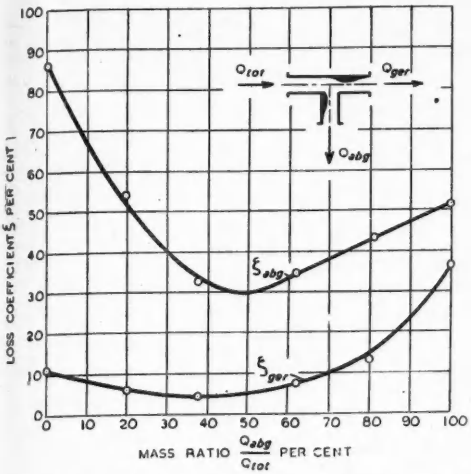

Fig. 7. **Loss coefficient against mass ratio 90 deg. branch, with flow guides.**

The frictional losses :

In the branched off channel :

$v = 0.6 \times 10 = 6$ m./sec.

$q = 1.94$ kg./m².

$R_e = 0.6 \times 0.185 \times 10^6 = 0.111 \times 10^6$

log $R_e = 5.045$, from Fig. 4,

$\lambda = 0.024$

$$\delta_R = 0.024 \times \frac{5}{0.3} \times 1.94 = 0.779 \text{ kg./m}^2$$

In the straight channel :

$v = 0.4 \times 10 = 4$ m./sec.

$q = 0.863$ kg./m²

$R_e = (0.185 - 0.111)\ 10^6 = 0.074 \times 10^6$, log $R_e = 4.869$, and from Fig. 4,

$$\lambda = 0.03;\ \delta_R = 0.03 \times \frac{5}{0.3} \times 0.863 = 0.432 \text{ kg./m}^2.$$

The total losses are : in the branched off channel 4.779 kg./m², and in the straight channel 1.228 kg./m².

INVESTIGATION OF THE ISOTHERMAL VISCOSITY OF BEARING ALLOYS

By J. De Lacombe & M. Dannenmuller. (From *Revue de Métallurgie*, Vol. 41, No. 3, 1944, p. 71–82).

This investigation is concerned with the plastic flow of bearing alloys in compression, particular attention being paid to the time factor. The machine employed for carrying out the tests is of a special design (Fig. 1) based upon experiences made in the creep testing of steels at high temperatures. The machine is equipped with a recording device which automatically charts the deformation of the test piece throughout the entire duration of the test run. A device for heating the specimen during the test at temperatures up to 1100 deg. C. is also provided. The heating coil (Fig. 2) is thermostatically controlled, so that the temperature of the specimen can be maintained constant with an accuracy of 0.1 deg. C. In the series of tests referred to below the employment of the heating device was confined to maintaining a uniform temperature of 40 deg. C. The recording device, comprising an optical extensometer with photographic registration, was adjusted to chart deformations of the order of 1.0–2.0 per cent, with an average test duration of 200 hours.

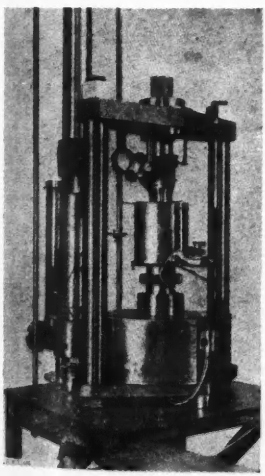

Fig. 1. **Testing Machine.**

The maximum compression load applied did not exceed 20 kg. per sq. mm. Prior to the test runs proper, the test pieces were subjected to a compressive load of 0.7 kg. per sq. mm. The test pieces were in the shape of machined castings of 25 mm. diameter and 50 mm. length. The shape and dimensions of the mould used for casting the specimens are given in (Fig. 3).

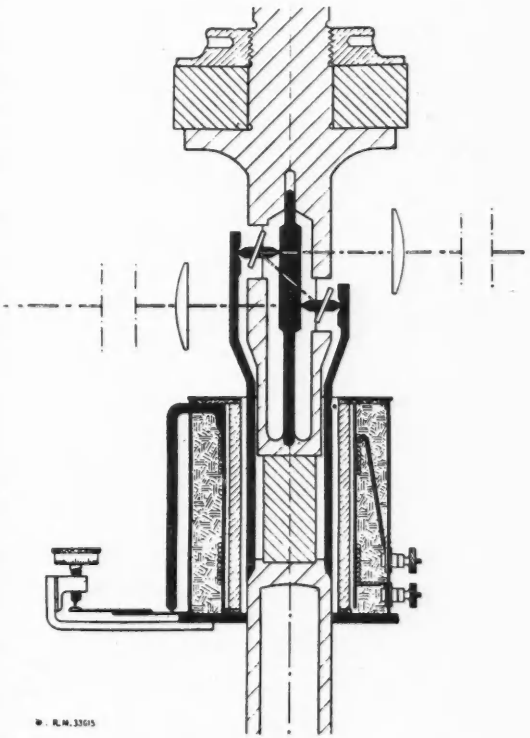

Fig. 2. **Detail of Testing Machine.**

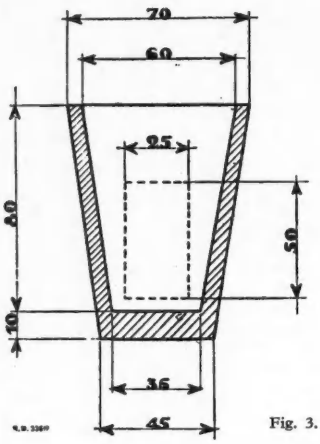

Fig. 3. Mould

A first series of test runs was concerned with determining the load *vs.* time characteristics for a final deformation of 1.0 per cent. The results of these tests are charted on the semi-log. basis as shown in (Fig. 4), where the compression loads producing 1.0 per cent deformation are plotted against the logarithm of the time. That long-time deformation characteristics may be quite different from short-time results is evidenced by (Fig. 5). Here it is seen that the alloy represented by the straight line (1) requires a greater compressive loading than that represented by the straight line (2) to exhibit a deformation of 1.0 per cent after one hour of loading, while the position is completely reversed after 200 hours. Only where alloys of similar compositions are concerned approximately parallel characteristics will obtain as shown in (Fig. 6).

On the other hand, there are also certain alloys which do not exhibit this kind of flow *vs.* time characteristic ; in these an initially high rate of plastic deformation diminishes to zero after a very short time of loading. Within a range of deformations from zero to 0.5 per cent, the compression *vs.* time characteristics resemble the creep characteristics of steels subjected to tensile stress at elevated temperature. Thus the rate of compressive deformation may either accelerate, or it may remain constant, or it may also begin to accelerate after a certain length of time. Characteristics of the latter type, as exemplified by (Fig. 7), are of particular interest as they emphasize the similarity of tensile and compressive behaviour. In the case of tensile tests the final acceleration of the rate of deformation has sometimes been explained by the fact that the ensuing reduction in area increases the specific stress under constant loading. Doubtless, this explanation may be helpful in certain cases, but it cannot be considered as fully satisfactory. This is proven by the fact that an acceleration in the rate of deformation may also occur in the compression test, that is to say, under conditions in which deformation actually serves to increase the loaded area. It must therefore be concluded that an acceleration in the rate of deformation may occur independently of the specific loading per unit of cross-sectional area.

That the similarlity of compressive and tensile deformation characteristics is by no means solely qualitative, is shown by the fact that both types of plastic deformation can be expressed by a function of the type : $\epsilon = \epsilon_o + a\,t^m + b\,t^n$. This goes to show that the mechanisms of compression and elongation are essentially similar in nature.

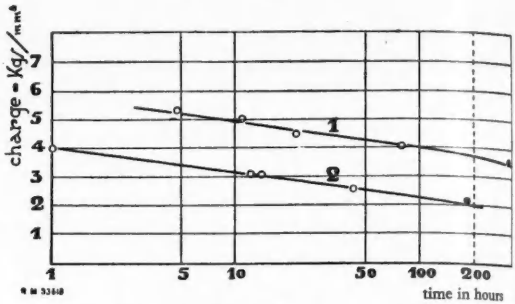

1. Alloy Pb = 73.5, Sn = 10, Sb = 15, Cu = 1.5.
2. Alloy Pb = 28, Sn = 60, Sb = 10, Cu = 2.0.

Fig. 4. Typical deformation characteristics.

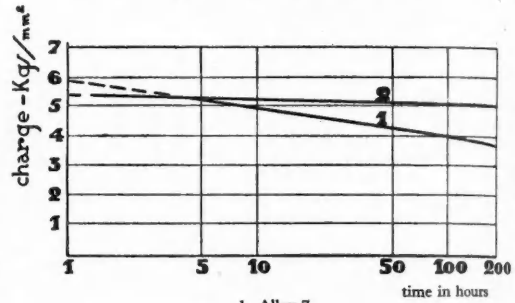

1. Alloy 7
2. Alloy 25

Fig. 5. Difference between long-time and short-time characteristics.

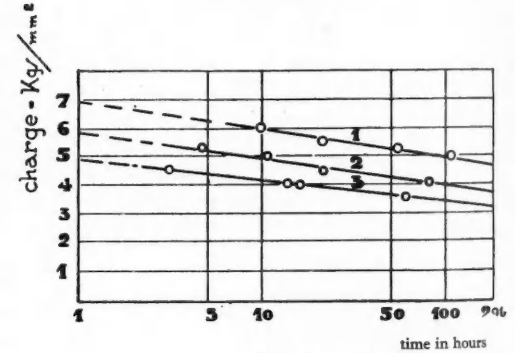

		Pb	Sn	Sb	Cu
1	.. ..	78.5	10	10	1.5
2	.. ..	73.5	10	15	1.5
3	.. ..	68.5	10	20	1.5

Fig. 6. Characteristics of similar alloys.

Each one of the alloys investigated was subjected to a series of tests at different loadings, and the results were utilised to establish the characteristic deformation coefficients $\frac{\epsilon_o}{\epsilon_{200}}$, m and n.

TIN-BASE ALLOYS.

The softest of the tin-base alloys listed in the subjoined Table I is alloy No. 1, containing 94 per cent Sn, 4.0 per cent Sb and 2.0 per cent Cd.

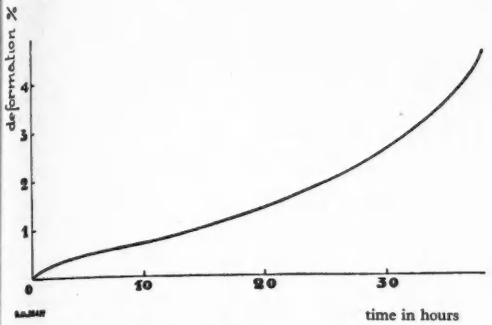

Alloy 15: Sn = 60, Pb = 28, Sb = 10, Cu = 2.
Fig. 7. **Accelerated characteristics.**

TABLE I.—TIN-BASE ALLOYS.

No.	Composition, % Sn	Sb	Cu	Cd	Specific Stress kg./sq. mm.	Coefficients of plastic flow ϵ_0 / ϵ_{200}	m	n
1	94	4.0	—	2.0	1.9	0.00	0.5 —0.6	1.2—1.4
2	90	6.5	3.5	—	3.2	0.10	0.8 —1.0	—
3	83	11.0	6.0	—	3.5	0.10	0.78—0.82	—
4	78	13.0	9.0	—	3.7	0.10	0.65—0.75	—

The specific stress required to produce 1.0 per cent deformation of this material in 200 hours is seen to be 1.9 kg. per sq. mm. The rate of deformation is substantially in linear relationship with the loading time, but a slight acceleration becomes noticeable after some 30 hours. The small initial elastic deformation accompanying the application of the load is completely recovered upon unloading, and the deformation characteristic resembles the straight line (4) plotted in Fig. 8.

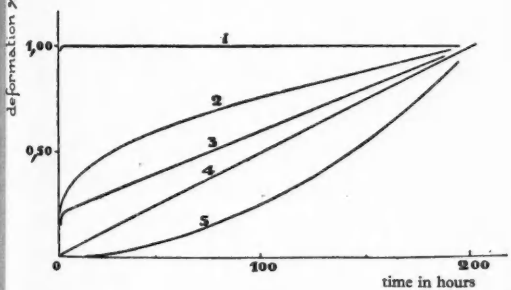

	ϵ_0 / ϵ_{200}	m
1	1.00	—
2	0.20	0.50
3	0.20	1.00
4	0.00	1.00
5	0.00	2.00

Fig. 8. **Typical characteristics.**

In cadmium-free tin-base alloys the specific stress required to produce 1.0 per cent deformation in 200 hours is raised by increasing the antimony percentage of the alloy and introducing approximately proportionate amounts of copper. Thus, for instance, alloy No. 2 containing 90 per cent tin, 6.5 per cent antimony, and 3.5 per cent copper, requires a specific stress of 3.2 kg. per sq. mm. It has an almost rectilinear deformation *vs.* time characteristic with an initial deformation of about one-tenth of the final deformation. According to its deformation coefficient (m = 0.8 — 1.0), the characteristic of this alloy will fall halfways between the characteristics (3) and (4) given in Fig. 8. Alloy No. 3 which contains 11.0 per cent of antimony and 9.0 per cent of copper has a still higher specific compression stress of 3.7 kg. per sq. mm.

LEAD-BASE ALLOYS.

The lead-base alloy No. 5 with 0.25 per cent cadmium and 0.75 per cent bismuth, listed in Table II, is the softest of all alloys tested. Its flow rate decreases during the first hour of loading, and then remains constant for more than 100 hours. The influence of different alloying constituents upon the plastic flow of lead-base alloys was systematically studied by using the flow characteristics of alloy No. 7 as basis of comparison. This alloy has a compressive strength of 3.4 kg. per sq. mm., and from the aspect of compressive strength is therefore comparable to a tin-base alloy. According to the data listed in Table II, copper additions tend to produce a slight increase in the compressive strength, while cadmium additions have the opposite effect. Table II also shows that a tin content of 10 per cent constitutes the optimum percentage from the aspect of compressive strength.

TABLE II.—LEAD-BASE ALLOYS.

No.	Composition, % Pb	Sn	Sb	Cu	Cd	Bi	Specific Stress kg./sq. mm.	Coefficients of plastic flow ϵ_0 / ϵ_{200}	m
5	98.25	—	0.75	—	0.25	0.75	1.1	0.15	1.0
6	74.2	10.0	15.0	0.8	—	—	3.4	0.20	0.45—0.50
7	73.5	10.0	15.0	1.5	—	—	3.4	0.20	0.50—0.60
8	72.0	10.0	15.0	3.0	—	—	3.7	0.25	0.48—0.53
9	78.5	5.0	15.0	1.5	—	—	3.1	0.25	0.45—0.50
7	73.5	10.0	15.0	1.5	—	—	3.4	0.20	0.50—0.60
10	63.5	20.0	15.0	1.5	—	—	2.4	0.15	0.55—0.75
11	78.5	10.0	10.0	1.5	—	—	2.9	0.20	0.45—0.60
7	73.5	10.0	15.0	1.5	—	—	3.4	0.20	0.50—0.60
12	68.5	10.0	20.0	1.5	—	—	4.4	0.20	0.60—0.70
13	70.5	—	—	1.5	3.0	—	2.6	0.20	0.55—0.65

The characteristics of viscous flow are seen to be but little influenced by variations in the percentages of the alloying constituents. Compared to the behaviour of the tin-base alloys, the viscous deformation of the lead-base alloys is more pronounced in the initial stages, but tends to slow down more markedly in the later stages. On the whole the deformation characteristics of lead bearing alloys are well represented by curve (2) in Fig. 8.

LEAD-TIN-BASE ALLOYS.

Two typical compositions of this class of alloys are given in Table III.

TABLE III.—MIXED ALLOYS.

No.	Composition, % Sn	Pb	Sb	Cu	Specific Stress kg./sq. mm.	Coefficients of plastic flow ϵ_0 / ϵ_{200}	m	n
14	56.5	33.5	6.5	3.5	1.5	0.00	0.25—0.30	1.00—1.25
15	60.0	28.0	10.0	2.0	1.5	0.05	0.70—0.90	2.80

These alloys are characterised by a low fusion point and small compressive strength. Under compressive load the rate of viscous deformation tends to increase. This tendency, which is particularly pronounced in the case of alloy No. 15, does not, however, make itself felt within the range of deformations considered permissible in practice; it is therefore of little importance.

CADMIUM-BASE ALLOYS.

The three cadmium-base alloys listed in Table IV are seen to offer considerably greater resistance to plastic deformation under compressive stress than either tin- or lead-base alloys. The time *vs.* plastic deformation characteristics of cadmium-base alloys generally range between the curves (4) and (5) of Fig. 8.

TABLE IV.—CADMIUM-BASE ALLOYS.

Composition, %				Specific Stress kg./sq. mm.	Coefficients of plastic flow		
No.	Cd	Cu	Ni		$\epsilon_0 / \epsilon_{200}$	m	n
16	98.7	1.3	—	5.5	0.00	0.50—0.70	2.5—3.0
17	97.0	3.0	—	6.1	0.15	0.50—0.65	—
18	98.6	—	1.4	6.2	0.05	0.50—0.55	2.0—3.0

ZINC-BASE ALLOYS.

Only one of the zinc-base group of alloys was investigated. Its composition is given in Table V, where it will also be seen that this type of bearing alloy shows a greatly superior resistance to plastic deformation as compared to any of the various alloy groups discussed above. The decrease in the plastic deformation rate of this alloy is not much greater than that experienced with the lead-base alloys. But its initial deformation is considerable. This is explained by the high compressive load required to produce 1.0 per cent deformation in 200 hours and also by the small modulus of elasticity of zinc-base alloys.

TABLE V.—ZINC-BASE ALLOYS.

Composition, %				Specific Stress kg./sq. mm.	Coefficients of plastic flow	
No.	Zn	Pb	Cu		$\epsilon_0 / \epsilon_{200}$	m
19	91	5	4	9.7	0.50	0.45—0.50

COPPER-BASE ALLOYS.

In the case of these alloys the rate of viscous flow is negligibly small, at least under loads producing a deformation of 1.0 per cent in 200 hours. As a matter of fact, this percentage is already reached in the initial stage, and one can say that the plastic limit lies above the elastic limit of the short-time test. The deformation characteristics of this group of bearing alloys therefore resembles characteristic (1) of Fig. 8.

TABLE VI.—COPPER-BASE ALLOYS.

Composition, %					Specific Stress kg./sq. mm.	$\epsilon_0 / \epsilon_{200}$
No.	Cu	Pb	P	Sn		
20	86.0	14.0	0.05	—	5.4	1.00
21	72.0	28.0	0.05	—	5.4	1.00
22	92.0	—	—	8.0	18.7	1.00

Referring to Table VI, it will be noted that the alloys No. 20 and No. 21 have identical compressive strength, and this in spite of the fact that the lead percentage of No. 21 alloy is twice that of No. 20 alloy. In these two alloys plastic deformation under the proof stress comes to an end within one hour after application of the load; but in the case of an alloy containing 92 per cent copper and 8 per cent tin (No. 22) viscous flow ceases even after as little as 30 minutes, although the compressive stress required is as large as 18.7 kg. per sq. mm.

MAGNESIUM-AND ALUMINIUM-BASE ALLOYS.

A number of magnesium-base and aluminium-base alloys are listed in Table VII.

TABLE VII.—ALUMINIUM- AND MAGNESIUM-BASE ALLOYS.

Composition, %							Specific Stress kg./sq.mm.	Coefficients of plastic flow	
								$\epsilon_0 / \epsilon_{200}$	m
No.	Mg	Pb	Al	Zn	Mn				
23	82.0	18.0	—	—	—		5.5	1.0	—
24	86.7	—	3.0	10.0	0.3		6.9	1.0	—
	Al	Pb	Sn	Sb	Cu	Mg			
25	99.7	—	—	—	—	—	4.7	0.80	—
26	92.0	2.0	2.5	3.5	—	—	6.2	0.50	0.50
27	93.0	—	3.5	—	—	3.5	13.7	1.00	—
28	90	—	3.0	—	4.0	3.0	19.7	1.00	—

Compression test conducted on the No. 23, 24, 27, and 28 alloys showed that the plastic deformation attains its final value within one or two seconds after application of the load. No additional deformation could be produced by keeping the test pieces under load for several hundred hours. In the case of the specimen No. 25 consisting of commercially pure aluminium a certain amount of plastic flow was found to persist up to the very end of the 200 hour period. But even so, 80 per cent of the total deformation of 1.0 per cent was produced within a few seconds after application of the load. The aluminium alloy No. 26 was found to exhibit a different behaviour in so far as only 50 per cent of the total deformation was produced instantly upon application of the stress.

As was stated before, all tests were conducted at a temperature of 40 deg. C. This temperature is below the temperature range usually encountered in actual bearings. Additional tests at higher temperatures have shown that the magnitude of the specific compression stresses required to produce 1.0 per cent deformation in 200 hours is substantially affected by a temperature increase. This goes to explain why the stresses given above are higher than the design stresses used in practice.

APPROPRIATE METHOD FOR FINDING THE SHEAR CENTRE POSITION OF A SINGLE-CELL WING NOSE BEAM

By E. PLÜSS, Publication of the Department of Aircraft Stressing, Swiss Federal Technical College.

(From *Flugwehr und Technik*, July, 1944, No. 7, pp. 202-203).

To calculate the torsional strength of wing nose-beams the knowledge of the shear centre position is required. The shear centre is that point through which the applied shear force must pass if the bending be unaccompanied by torsion. The simplifications consist in the assumption that the cross-sectional area of the wing spar flanges is concentrated at the intersections of the spar web with the wing cover, and further in neglecting the stringers. Then the shear flows over the nose as well as over the depth of the spar remain constant (Fig. 1).

SHEAR FLOW, SHEAR STRESS AND ANGLE OF TWIST.

For the correct estimate of the shear flow q (kg./cm.) and the shear stress $\tau = q/d$ (kg./cm²) by the generally used method, the knowledge of the shear centre position is not necessary while the torque $M = Q \cdot a$ is applied.

Thus: shear flow in cover

$$q_2 = \frac{M}{2F} = \frac{Q\,a}{2F} \text{ (kg./cm)} \quad \ldots \text{ Batho:-Bredt formula}$$

$$\text{Shear flow in spar web } q_1 = q_2 + \frac{Q}{h} \text{ (kg./cm.)}$$

The angle of twist of a wing-cell of the length l is

$$\varphi = \frac{M}{J_D \cdot G} \cdot l \text{ (radians)}$$

where

$$J_D = \frac{4F^2}{\frac{s}{d_2} + \frac{h}{d_1}} \text{ (cm}^4\text{)}$$

and G = modulus of shear (kg./cm²)

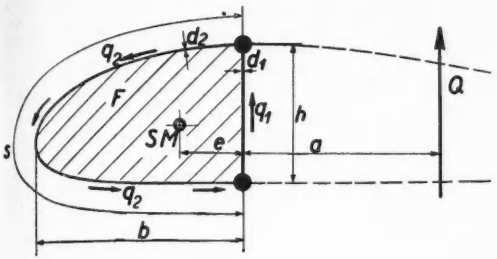

Fig. 1.
Notations : Q = shear force
SM = shear centre
d_1 = thickness of web
d_2 = thickness of cover
e = shear distance from web
h = spar depth
b = width of wing cell
s = developed length of covering skin

For variable J_D the angle φ can be found graphically by plotting $\frac{M}{J_D \cdot G}$ against l, and taking the area under this curve.

In calculating the angle of twist it is not indifferent where the shear centre is located. The torque M must be taken about the shear centre ; thus :

$$M = Q\,(a + e)\ (\text{cm./kg.})$$

THE POSITION OF THE SHEAR CENTRE.

For the above simplified assumptions the distance of the shear centre is given by

$$e = \frac{2\,\frac{F}{h}}{1 + \frac{s}{h}\,\frac{d_1}{d_2}}\ (\text{cm.})$$

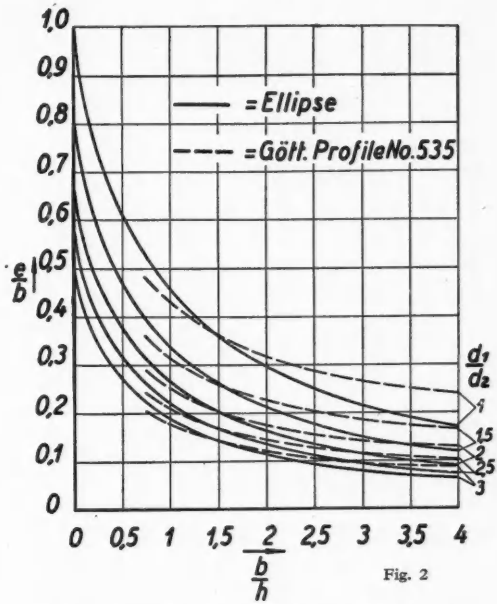

Fig. 2

By using this equation, e has been calculated for the aerofoil section Göttingen 535 (a section often employed in glider design) and is plotted in a non-dimensional form in Fig. 2. For comparison, the shear centre distance for a semi-elliptic section is plotted too. It can be seen that for a certain $\frac{b}{h}$ – ratio there is close agreement and for such cases e can be read of the graph for the ellipse and F and s need not be determined by measurement.

DIESEL FUELS

From PROFESSOR T. M. MELKUMOV's Book, *Theory of the High-Speed Diesel*, Moscow, 1944, pp. 332-340 and 347-352.

SLOW speed diesels of the stationary and the marine types do not require any special quality of diesel fuel, but will give satisfactory service with a wide range of oils. In the case of high speed diesels, however, requirements are much more exacting. This is mainly due to the fact that because of the high engine speed, less time is available for combustion of the fuel ; in fact, the available time is only one-tenth to one-twentieth of that available in the slow speed diesel. Moreover, the dimensions of the fuel injection system are much smaller in the case of the high speed diesel as compared to the slow speed type. Furthermore, in automobile and tractor diesels, less viscous types of fuel are used.

In aviation diesels the severe operating conditions and the requirements of highest service reliability make it essential that only fuels of highest quality should be used. In Germany where naphtha-base fuels must be imported, high speed diesels of the ante-chamber type for land transport purposes are operated on oils derived from coal, but for aviation diesels only naphtha-base oils are used.

The specific gravity of naphtha generally ranges from 0.8 to 0.9, but specially light naphthas of a specific gravity of 0.73 and particularly heavy naphthas of 0.97 specific gravity also exist. Salient data on a few typical naphtha fractions are given in Tables I and II.

As aviation diesels must reliably operate in widely different climates, the fuel must possess sufficient fluidity at low temperature. Consequently, the freezing point of aviation diesel fuel must be below the lowest air temperature that can be expected to occur during the cold season or in the Northern regions that may have to be traversed. Furthermore, the fuel must be well filtered in order to avoid choking of the nozzles and rapid wear of pump and nozzles. This calls for a low viscosity fuel such as gas oil, mixtures of gas oil and kerosene, or neat kerosene. Kerosene and particularly gas oil possess sufficient oiliness to ensure reliable operation of the injection system.

Gas oil and kerosene have different chemical structures according to the naphtha from which they are derived. For aviation diesels a fuel is used which is derived from a specified range of naphthas and which possesses a particularly high ignitability.

The specific gravity is an important characteristic of the fuel. In the case of gas oil it varies within the range of 0.84–0.88, and in the case of kerosene between 0.82 and 0.836. If the temperature of the fuel is other than 20 deg. C., the variation in specific gravity with the temperature can be found from

$$\gamma_{20} = \gamma_T + 0.00068\ (t - 20)$$

TABLE I.

No	Type of fuel	Spec. Gravity	Ult. Analysis C	Ult. Analysis H	Lower Cal. Value Kcal./kg.	Distillation test: Initial Boiling Point, deg. C.	Distillation test: Recovery, per cent up to 250	up to 300 deg. C	up to 350	Flash Point deg. C.	Fire Point deg. C.
1	Gas oil (Balakhany)	0.9003 (15 deg. C.)	86.6	12.5	10,290	161	4.0	31.0	48.6	100	132
2	Gas oil (Balakhany naphtha base)	0.9057 (20 deg. C.)	—	—	—	266	—	30.5	76.5	124	—
3	Gas oil (Bibi-Eybat)	0.85 (15 deg. C.)	86.65	13.58	10,431	—	23.2	75.3	82.2	64	90
4	Gas oil (Bibi-Eybat light)	0.8828 (15 deg. C.)	87.47	12.52	10,133	235	—	—	93.0	113	—
5	Gas oil (Kara-chu-kur)	0.8615 (20 deg. C.)	—	—	—	260	—	29.0	86.0	126	—
6	Gas oil (Binagadin)	0.891 (15 deg. C.)	86.5	12.5	10,270	—	17.0	54.6	67.2	69	103
7	Gas oil (Binagadin)	0.826 (20 deg. C.)	—	—	—	196	—	—	347 deg. 94.0	74	—
8	Gas oil (Surakhany)	0.846 (15 deg. C.)	85.6	13.4	10,429	153	28.6	70.1	75.7	67	90
9	Gas oil (Surakhany)	0.84 (20 deg. C.)	—	—	—	219	—	69.0	335 deg. 94.0	91	—
10	Gas oil (Grozny)	0.8382 (20 deg. C.)	—	—	—	205	—	50.5	89.5	78	—
11	Gas oil (Dossor)	0.869 (15 deg. C.)	86.35	13.46	10,216	213	—	—	86.5	96	—
12	Kerosene (Grozny Par. Naphtha base)	0.823 (15 deg. C.)	86.4	13.70	10,306	146	24.7	79.7	99.7	80	98
13	Kerosene (Dossor)	0.8481 (15 deg. C.)	84.79	14.03	10,265	166	—	—	98.0	44	—
14	Kerosene (Tractor No. 1 brand)	0.826 (20 deg. C.)	—	—	—	up to 270 deg. —10%	up to 270 deg. 80.0%	98.0	—	28	—

TABLE II.

Type of fuel	Spec. Gravity at 20 deg. C.	Initial Boiling Point deg. C.	Distillation temperatures, deg. C. 10%	20%	40%	50%	60%	80%	90%	95%	97%	98%	End Point deg. C.
Aviation benzine B–78	0.70	Not less than 40°C.	82	—	—	95	—	—	110	—	130	—	130
Aviation benzine B–70	0.73	Not more than 65°C.	88	—	—	106	—	—	138	—	—	170	170
Aviation cracking benzine KB–70	0.72	35–45	70	—	—	110	—	—	145	—	175	—	175
Benzine E light, Grozny, motor benzine	0.725	Not more than 50°C.	—	—	100	—	—	—	160	96% at 175°C.	—	—	175
Benzine E light, Baku, B, motor benzine	0.75	Not more than 80°C.	—	25% at 100°C.	—	—	—	—	—	170	—	—	180
Ligroin	Not more than 0.795	—	12% at 150°C.	—	—	—	—	—	200	—	—	230	230
Kerosene tractor Brand No. 1	Not less than 0.826	—	175	—	—	—	—	270	—	—	—	300	300
Gas oil E, Grozny	Not less than 0.835	—	—	—	—	—	300	—	—	360	—	—	360
Gas oil E, Baku	Not more than 0.876	—	—	—	—	—	300	—	—	—	—	—	360
Solar oil	0.87–0.89	250–270	—	23% at 300°C.	—	—	—	360	—	—	—	—	400

The heat balance of diesels must be based upon the lower heating value of the fuel, as the products of combustion leave the engine at a high temperature, so that the latent heat of the water vapour is not recovered. The lower cal. value of gas oil and kerosene amounts to 10,200–10,500 Kcal. per kg. According to their ultimate analysis, solar oil, gas oil and kerosese contain from 85.5–86.5 per cent carbon, 13.0–13.5 per cent hydrogen, and other constituents not exceeding 1.0–2.0 per cent. Knowledge of the ultimate analysis is essential in the evaluation of engine tests. The viscosity of aviation fuel must lie within the range of 1.2–2.0 deg. Engler at 20 deg. C. and between 2.0 and 4.0 at 0 deg. C.

The composition of the fuel on the basis of fractions has long been recognised as an important factor of the combustion process in Otto engines ; while in the case of high speed diesels fractional composition was thought to be less important, as it was believed that the fuel is not given sufficient time to evaporate and therefore must burn in the liquid phase. But it has now been established that in high speed diesels different fuels of identical specific gravity but of different fraction percentages exhibit different combustion characteristics in the engine. For this reason present day fuel standards include stipulations with regards to the required fraction percentages. In the case of aviation diesels the stipulations are as follows :

Commencement of distillation : 180–220 deg. C. and not higher than 230 deg. C.

10% point of distillation : not higher than 240 deg. C.

60% point of distillation : not higher than 300 deg. C.

95% point of distillation : not higher than 360 deg. C.

The flash point of an oil is defined as the temperature at which a sufficiently large quantity of low-boiling constituents has been evaporated to form a combustible mixture with the air on the surface of the fuel which will ignite momentarily upon application of a flame. At this temperature the speed of evaporation is insufficient to maintain combustion, and the flame is therefore extinguished after flashing has taken place.

The fire point is determined as the temperature at which combustion continues after flashing. Neither flash point nor fire point characterise the behaviour of the fuel in the engine, but are only a measure of the danger of fire. The higher these temperatures, the less likely is the fuel to catch fire. The flash point of petrol is —25 deg. C. and less, and that of gas oil is +65 deg. C. and more. The presence of water in the fuel is undesirable for various reasons. First of all, water reduces the heating value of the fuel per unit of weight. Secondly, the evaporation of the water content decreases the available heat content of the fuel. The presence of water in the fuel may also lead to the occurrence of corrosion in the injection system. In the cold season it may also cause the formation of ice in the fuel system and thus interrupt the fuel supply to the engine. The presence of a small amount of water in the fuel has, however, no harmful influence upon the combustion process ; and the presence of water vapour in the air, or a small admixture of water to the fuel, will even have a beneficial catalytic effect upon the oxidation of the carbon.

The presence of foreign bodies in the diesel fuel cannot be tolerated as it causes wear of the fuel pump and of the nozzles ; foreign bodies may also choke the nozzles. In order to eliminate any impurities present in the fuel, filters must be used. The sulphur content of benzine, kerosene, and gas oil does not usually exceed 0.05–0.15 per cent; but in certain naphthas and naphtha products larger sulphur percentages are sometimes encountered. The presence of sulphur in the fuel is not, however, harmful ; and tests conducted with fuels of sulphur contents as high as 2 per cent have shown that the operation of the engine remains unaffected. Nor could it be established that the presence of sulphur in combination with the presence of water is harmful to either combustion chamber or cylinder surface. Ash, if allowed to be present in considerable amounts, will cause wear of the fuel injection system and of the cylinder surface. In diesel fuel the ash content must not therefore be larger than 0.01 per cent by weight.

The cold point is defined as the temperature at which the fuel will cease to flow. In the case of aviation diesels this temperature should lie at —40 to 50 deg. C. or even —50 to 60 deg. C.

THE MOTION RESISTANCES OF RAILWAY VEHICLES AND THE TRACTIVE RESISTANCE OF THE BROWN BOVERI GAS TURBINE LOCOMOTIVE

By A. E. MÜLLER. (From *The Brown Boveri Review*, June, 1944, p. 200-205)

GENERAL FACTS CONCERNING THE MOTION RESISTANCE OF RAILWAY VEHICLES.

GREAT diversity exists between the data and formulae given in text books and technical publications for the tractive resistance of trains. The values given differ very greatly according to railway practice in Europe, England and America.

The majority of the formulae to be found in publications are no longer adequate for the present standard of railway locomotive construction. Only test data obtained *with modern* rolling stock is of practical importance nowadays. Extensive and very systematic measurements have recently been made on *trains without locomotives* by the German State Railway ; the results of these measurements are to be found in the technical press* Up to the present there are unfortunately only very few data available for the tractive resistance of *locomotives*.

This fact combined with interest in individual-axle drive resulted in special test runs for determining the tractive resistance of the Brown Boveri gas turbine locomotive†. These test runs were rendered possible by the Swiss Federal Railways placing their dynamometer car at our disposal and actively co-operating with us during the tests.

The *tractive resistance* with which this article is concerned, is only part of the resistance which occurs when moving at a constant speed. The following table shows the various resistances which compose the motion resistance :—

Rolling Resistance resulting from :—rotational friction of axle journals : rolling friction between wheel rims and rails ; effects of oscillations and concussion (w_T)	**I Tractive Resistance** (w_O)	**Motion resistance at a constant speed on a tangent level track in still air** (w)
Air Resistance (w_1)		
Resistance due to Grades (w_S)	**II Track Resistance**	
Curve Resistance (w_K)		

Group I includes all resistances which are directly and inseparably concerned with the motion of the vehicle (tractive resistance), whilst the resistances of group II are additional resistances which depend on the condition and nature of the track (track resistances).

The *tractive resistance* can vary very greatly depending on the condition of the track, design and heating of the bearings, weather conditions, and also other influences of various kinds. The arrangement of the axles and the form of the vehicles is also of great importance ; furthermore the fact that certain inaccuracies are unavoidable with all practical methods of measurement. Therefore, no extreme degree of accuracy is to be expected from the coefficients of the resistance formulae and this also accounts for the deviation occurring in the measured values and the great differences between data given in publications concerning such measurements. The motion resistance is generally referred to a weight of 1 ton (separate for the locomotive and the train without locomotive). The *specific value* in kg./t of the tractive resistance is also termed " locomotive resistance " or " train resistance " (kg./t. or lbs. per ton) in railway literature.

METHOD OF MEASUREMENT.

The most expedient method is *to measure the tractive effort directly at a constant speed*, whereby the tractive effort of the locomotive and the tractive resistance are in equilibrium. The tractive effort at the draw-bar of the locomotive, that is the actual value of the *tractive resistance of the train without the locomotive* is thus determined by the dynamometer car coupled to the locomotive. A direct measurement of the tractive effort required to move the *locomotive alone* is thus not possible by this means. It can, however, be found by measuring the current, because there is a definite relationship between the tractive force at the tread and the torque and current of the traction motors according to the characteristic

*Sauthoff : " Die Bewegungswiderstände der Eisenbahnwagen unter besonderer Berücksichtigung der neueren Versuche der deutschen Reichsbahn." *Diss. T.H.*, Berlin, 1933.
Vogelpohl : " Die physikalische Natur der Bewegungswiderstände von Eisenbahnfahrzeugen." *ZVDI*, Vol. 79, No. 28, 1935.

†See detailed description of the gas turbine locomotive in *The Brown Boveri Review*, No. 5, May, 1942.

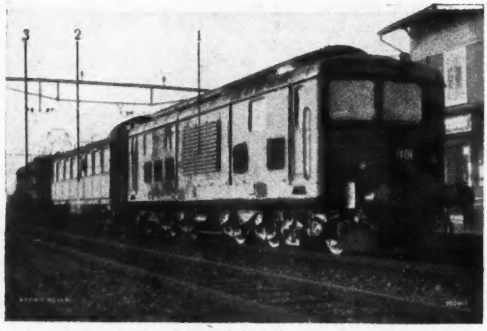

Fig. 1. Test train for determining the tractive resistance of the Brown Boveri gas turbine locomotive.
1. Gas turbine locomotive. 2. Dynamometer car. 3. Electric locomotive.

curves of the motors determined on the test bench. If this method is applied to locomotives alone, it is to be noted that the air resistance conditions at the rear of the locomotive are not the same as when coaches are coupled to the locomotive. The rear suction increases the tractive resistances. In practice such measurements are accompanied by certain difficulties due to the small powers which have to be exerted at the tread when running on a level track and because straight stretches of track with large gradients, which would require the expenditure of larger powers, only occur very rarely.

In the case of the gas turbine locomotive it is possible to apply this measuring method due to the fact that a single traction motor can be supplied with the Diesel generator set for starting the gas turbine plant, thus enabling the locomotive to be driven on the level at constant speeds up to 25 km./h. A large number of measurements were made according to this method and these are for the slow speed range (approx. 3–25 km./h.), a very valuable addition to the main measuring method subsequently described.

A *combined method* was used to determine the tractive resistance of the gas turbine locomotive, whereby during constant speed over a straight horizontal track the tractive effort at the tread was determined by current measurements and the tractive effort at the drawbar by the dynamometer car. The tractive resistance of the locomotive alone is obtained from the difference of these two tractive efforts. The train used for these tests was composed of the gas turbine locomotive, the dynamometer car and an electric locomotive as the "load locomotive" (Fig. 1). The measurements were made under conditions which in every respect correspond to those actually existing in practice, because the dynamometer car and the "load locomotive" replace the coaches.

TEST RUNS.

The choice of a suitable test track the correct constant speed and the certainty that the brakes on all the vehicles are fully released, is of great importance as regards the results of the measurements. The selected test track was the approximately 6 km. long Solothurn-Selzach line, lying in open country: there is no dense traffic on this line so that a certain amount of freedom was possible as regards the arrangement of the tests. The line includes an entirely straight horizontal stretch 1434 metres long over which constant speeds varying between 10 and 100 km./h. could be maintained without difficulty. The electric "load locomotive" was very useful for this purpose, because, together with the gas turbine locomotive, it enabled the test train to be accelerated to the desired speed in a very short time and also served to regulate the speed rapidly to the desired constant value.

Measurements were made on the 8th and 9th of December, 1942, under the following conditions:—

Gas turbine locomotive data (*Fig.* 2):

Gauge	1435 mm.
Weight	93 tons
Wheel arrangement	1 A – Bo – Al
Head form	rounded
Cross-sectional area	11 m²
Driving wheel diameter with tyres in new condition	1230 mm.

(Since up to the time the test runs were made the locomotive had only covered a distance of 2000 km. it can be assumed that the diameter of the driving wheels was still 1230 mm.).

4 traction motors driving the axles over Brown Boveri spring drives.

Transmission ratio of gears	1 : 4.53
Gear efficiency	97.5 per cent

Weight of test train:

Gas turbine locomotive	93 tons
Dynamometer car	43 tons
Electric locomotive Ae 4/7 with recuperation	123 tons
Total weight	259 tons

Speed measurement:

By distance and time observations (100 metre marks along the track), Amsler speed indicator in the dynamometer car, tachometer on the gas turbine locomotive. (The correction factor for the readings was 0.95, that is tachometer reading divided by 0.95 = effective speed).

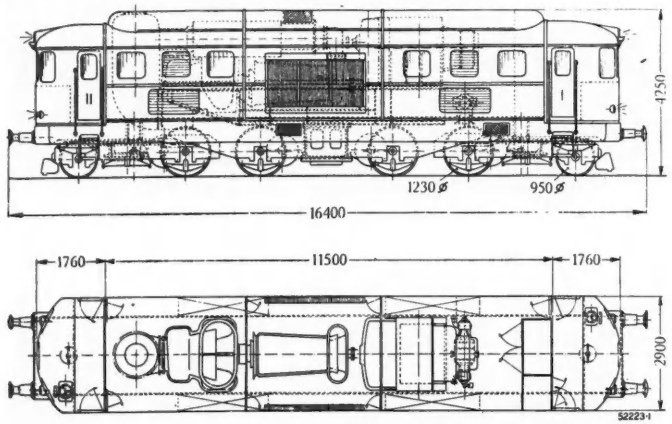

Fig. 2. Brown Boveri gas turbine electric locomotive type 1A-Bo-Al for 2200 h.p. continuous rating.
Service weight: 93 tons.
Axle pressure:
14.5 – 15.8 – 16 – 16.1 – 15.7 – 14.9.
Lateral clearance of axles in mm.:
± 140, ± 70*, ± 7, ± 10, ± 10, ± 7, ± 70*, ± 140.
*Pivots.

Weather on the 8th and 9th December, 1942 :

Foggy, calm, temperature 3.5–4 deg. C., air humidity 88 per cent, barometer reading 736 mm.

TEST RESULTS.

The figures obtained from the test runs of the 8th and 9th December, 1942, on the Solothurn-Selzach line were supplemented by test results obtained on a dynamometer car test run on the Basle-Zurich-Coire line (weather conditions the same as on 8th and 9th December, 1942), as well by results obtained from test runs previously undertaken on the locomotive alone driven by the Diesel generator set. The measured values show considerable scatter, due on the one hand to the unavoidable inaccuracy of all practical measuring methods, and on the other hand as a result of the differences in tractive resistance which actually occur due to external influences (bearing temperatures, condition of rails and overhead lines, air currents). In the velocity-tractive resistance diagram shown in Fig. 3 the measured points lie between the dotted limiting curves 1 and 2. The occurrence of the measured points is such that two average value curves corresponding to a condition of the locomotive with cold axle bearings and cold lubricating oil and warm bearings and warm oil, respectively, can be drawn. After about two hours running with reference to the bearings in the cold condition, a reduction in tractive resistance of about 20 per cent was ascertained. When applying the measured values from the test runs where the locomotive was driven by the Diesel generator set and a single traction motor, due consideration was paid to the fact that the other three driving axles were not " driving " but " driven," the " internal friction " of the " driven " axle drives being determined by calculation.

Curve $w_o = f(v)$ in Fig. 3 represents the *specific tractive resistance* of the gas turbine locomotive as an average value curve obtained from test results with the bearings in a warm running condition for a speed range of 20–100 km./h. This curve should prove a valuable addition to the data existing on the tractive resistance of modern locomotives with individual-axle drive, electrical power transmission, and a weight of about 100 tons.

At about 10 km./h. the tractive resistance is a minimum, this being due to the characteristic behaviour of the axle bearings. Below about 10 km./h. the tractive resistance increases rapidly because the lubrication of the slowly rotating axles deteriorates. When starting up from rest specific tractive resistance values of 8 to 15 kg./t. were obtained, depending upon the duration of the stoppage.

The average value curve obtained from tests and shown in Fig. 3 can be expressed by means of the formulae for calculating the resistance values ; at the same time some particulars concerning these resistance formulae are given.

For calculating the *absolute values* of the tractive resistance in kg. formulae of the following kind are generally used :—

$$W_o \text{ (in kg.)} = k_o \,.\, G + k_1 \,.\, v^2 \quad .. \quad .. \quad (1)$$

$$W_o \text{ (in kg.)} = k_o \,.\, G + k_2 \,.\, v \,.\, G + k_3 \,.\, v^2 \quad (2)$$

W_o = Tractive resistance in kg.
G = Locomotive weight in tons.
k_o = Empirical value for the specific rolling resistance, depending on the weight. This value is not to be considered as fixed.
k_1, k_3 = Empirical parameter for the air resistance, very greatly dependent on the shape of the locomotive.
k_2 = Additional factor due to uneven running (dependent on weight).
v = Running speed in km./h.

The factors k are detemined mathematically in such a manner that the results obtained by experience and

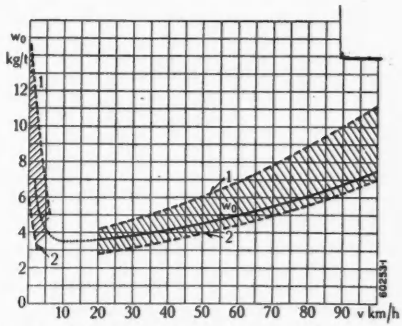

Fig. 3. **Specific tractive resistance of the Brown Boveri gas turbine locomotive.**
1 and 2 are upper and lower limiting curves for the plotted measured points.
w_0 (in kg./t.) = 3.5 + 0.0004 . v^2.

test runs can readily be reproduced in the form of curves. The binomial formula (1) has been in use in Europe for some time now, whilst in America the trinominal formula (2) is generally used.

It is usual and also very useful to use *specific values* (kg./t.) in the resistance formulae :

$$w_o \text{ (in kg./t.)} = k_o + \frac{k_1 \,.\, v^2}{G} \quad .. \quad .. \quad (1a)$$

$$w_o \text{ (in kg./t.)} = k_o + k_2 \,.\, v + \frac{k_3 \,.\, v^2}{G} \quad .. \quad (2a)$$

The binomial formula (1a) is selected to obtain an analytical expression of the average of the measured values, this being written as follows :—

$$w_o = k_o + k_1' \left(\frac{V}{10}\right)^2 \,.\, \frac{1}{G} \quad .. \quad .. \quad (3)$$

As regards the value of the air resistance in the formula for specific tractive resistance, it is to be emphasized that a " specific air resistance " in kg./t. is only a calculated value, because the absolute value of the air resistance is naturally independent of the weight.

According to the results the specific rolling resistance k_o of the gas turbine locomotive (rolling friction between wheels and rails + sliding friction in the axle bearings) amounts on the average to 3.5 kg./t. with warm bearings. The axle bearings are then not run in.

In the second term of the formula the parameter k'_1 for the air resistance includes the sectional area of the locomotive (F in m²) and an air resitance factor (c) which depends on the shape and condition of the surface ($k'_1 = F \,.\, c$). For the gas turbine locomotive F = approx. 11 m². According to data given in publications the air resistance factor c for a rounded locomotive head can be assumed to be 0.34. The results of the test runs with the gas turbine locomotive for a speed range of between 20 to 100 km./h. can thus be expressed by the *average value formula for the specific tractive resistance* as follows :—

$$\underline{w_o \text{ (in kg./t.)} = 3.5 + 0.0004 \,.\, v^2} \quad .. \quad (4)$$

COMMENTS AND CONCLUSIONS.

1. *Tractive resistance formulae with specific values* cannot be applied generally without restriction, this being especially the case when the resistance values of two locomotives of different construction or considerably different weight have to be compared. In order to be able to make comparisons it is essential that the re-

sistances should be expressed as absolute values in kg. The specific rolling resistance k_o in kg./t. vehicle weight, as the summation value of the rolling friction and axle bearing friction, is less with heavier vehicles than with light ones. The specific value of the bearing friction itself and with reference to 1 ton vehicle weight also decreases when the weight of the vehicle increases. This fact must be observed when designing large locomotives having several hundred tons service weight. For locomotives with *plain axle bearings* and a service weight of about 200 tons, k_o is estimated to be about 3 to 2.5 (down to 2) kg./t. Large locomotives are constructed in two or three units. This does not appreciably affect the *specific* tractive resistance of the locomotive as a whole, because the resistance at the end of the second and third units of the locomotive is small. For locomotives having 2 or 3 units it is expedient to make a correction for the air resistance factor c, the value k_o remaining unchanged. For a double-unit express streamlined locomotive the German State Railway uses a value of $c = 0.25$ and for a triple-unit locomotive $c = 0.30$.

2. Of late *roller axle bearings* are being used for motor-coaches, high-speed motor-coach trains and also locomotives. As regards resistance conditions, roller bearings possess the advantage that there is very little difference between the friction at rest and in motion. Friction at rest (starting up from a standstill) amounts to only about 5 per cent of that for plain bearings, according to particulars given by roller bearing firms. When running at higher speeds, however, roller bearings do not result in appreciable reduction in tractive resistance, due to the predominating influence of the air resistance.

3. The tractive resistance formula (4) for the gas turbine locomotive was determined during calm weather. The standard for resistance formulae should be calm weather. When carrying out tests a windless day should be chosen because this is the only possible way of obtaining a uniform air flow, which is essential when comparisons between various types of vehicles have to be made. If the timetable does not already contain allowances for unfavourable weather (wind), this is taken into account by making certain empirical additions to the speed. The maximum effect of the wind is not when there is direct head wind but when the wind comes from the side. Experiments made concerning the wind effect enable the following additions to be assumed :—

12–15 km./h. for moderate lateral winds.

20 km./h. for strong lateral winds.

30 km./h. for severe and continuous storms.

The value of any supplements which may have to be made must be decided in each particular case in view of an excessive dimensioning or poor utilization of the locomotive. For instance, for a moderate lateral wind, formulae (4) would be altered as follows :—

$$w_o \text{ (in kg./t.)} = 3.5 + 0.0004\,(v + 12)^2.$$

A NOVEL AUTOMATIC SYNCHRONIZER

By A. GANTENBEIN and J. JACKLE. (From *Bulletin Oerlikon*, No. 249, May/June, 1944, pp. 1599-1606.

THE working of the component parts of the new Ultra-rapid-Synchronizer is strictly in accordance with the underlying theoretical concepts, thus making it possible to effect synchronization with differences in frequency as large as 2 per cent and with switching times up to 0.5 seconds. The main components of this device are :

(*a*) a synchronoscope for determining the phase ;
(*b*) a differential measuring device for ascertaining the prevailing difference in frequencies ;
(*c*) a device for frequency equalisation.

The salient features of the synchronizer are shown in Fig. 1, where the synchronoscope (30) represents the phase-sensitive organ. The latter is designed as a two-pole motor, the stator being connected with the one, and the rotor with the other of the buses to be synchronised. If phase equality prevails, pointer (61) will point upward as shown in the illustration, but if the phases are in opposition, it will point downward. If the two frequencies are different, the pointer will rotate in the "fast" or in the "slow" direction indicating whether the machine to be synchronized is to be speeded up or slowed down. The speed with which pointer (61) and shaft (33) rotate is a direct measure of the difference in frequency prevailing.

Actual measurement of the difference in frequency is carried out with the employment of the electro-magnetic slip coupling (40) which consists of an U-shaped iron ring (43) and the armature (42). This armature is made of non-magnetic material, but is equipped with magnetic pole pieces. It is rigidly coupled with the gear (41). The latter is driven by the shaft (33) through the gear (32), a mechanical slip-coupling being installed between the shaft (33) and the gear (32). The aluminium rotor (45) which rotates in the air gap between the iron ring (43) and the armature (42) is carried on the shaft (46) to which the sheave (51) is also affixed. This sheave is engirdled by the two thin steel tapes (56), the free ends of which are attached to the tension springs (57). The operating principle of this mechanism is as follows :—

By passing a direct current through the coil (44), a magnetic field is created in the air gap and in the aluminium rotor. As the armature (42) is coupled with the synchronoscope by means of the gears (32) and (41), it will follow the rotation of the synchronoscope, and the eddy currents produced in the aluminium rotor will tend to rotate it in the same direction as the armature.

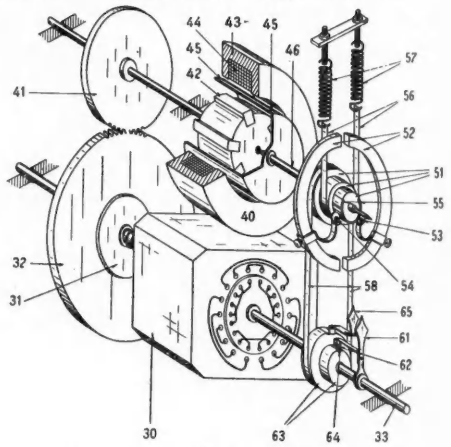

Fig. 1. **Axonometric representation of the Ultra-rapid-Synchroniser.**

(30) Synchronoscope.
(31) Mechanical slip coupling.
(32), (41) Gears.
(33) Shaft of synchronoscope.
(40) Electro-magnetic slip coupling.
(42) Armature.
(43) V-shaped iron ring.
(44) Field coil (d.c.).
(45) Aluminium rotor.
(46) Shaft.
(51) Sheave.
(52) Adjustable ring for blocking contacts.
(53), (54), (55) contacts.
(56), (58) Steel tape.
(57) Tension springs.
(61) Phase pointer.
(62) Roller contact.
(63) Sheave.
(64) Contact.
(65) Frequency differential pointer.

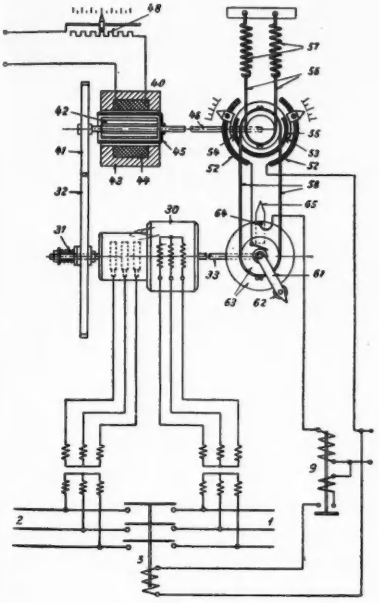

Fig. 2. **Principal circuits of Oerlikon-Ultrarapid-synchroniser.**

Such a rotation of the aluminium rotor is, however, opposed by the two helical springs (57) which exert a torque upon the rotor by means of the two steel tapes (56). This torque varies with the angle of rotation according to a straight line law, the actual slope of the characteristic depending upon the stiffness of the springs. The torque transmitted by the armature upon the aluminium drum is, however, also in direct proportion with the rotational speed of the shaft (33), provided that the current passing through the coil (44) is maintained constant. After rotation of the drum through a certain angle, a state of equilibrium between the electrical and the mechanical torque will therefore be established. Thus this angle will be a direct measure of the rotational speed of shaft (33), that is to say, of the difference in frequency prevailing.

Sheave (51) is coupled with sheave (63) by means of the two steel tapes (58), the latter sheave being freely rotatable upon the shaft (33) of the synchronoscope. The pointer (65), attached to sheave (63), gives a direct indication of any difference in frequency that may prevail. Sheave (63) also carries a contact piece (64) which makes contact with the roller-contact (62) when the pointers (61) and (65) are in identical position.

In order to ensure that closing of the switch can be effected only if the difference in frequency is within the permissable range, two additional contact pieces (53) and (54) are provided on sheave (51). These contacts are placed in series with the contacts (62) and (64), as shown in the basic circuit diagram given in Fig. 2. Here it is seen that closing of the contacts 53/55, 55/54 and 62/64 will cause an actuating impulse to be sent to the switch. The contacts 53/55 and 55/54 are placed in series so as to make it possible to select the frequency difference at which the closing impulse is to be given to the switch. This adjustment is effected by merely moving the contacts into the appropriate position.

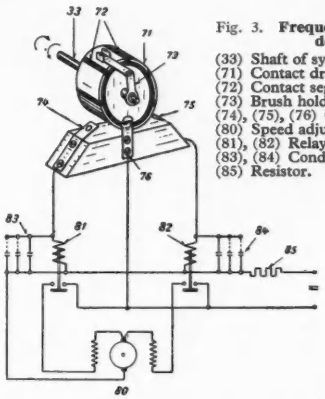

Fig. 3. **Frequency—equalisation device.**
(33) Shaft of synchronoscope.
(71) Contact drum.
(72) Contact segments.
(73) Brush holder.
(74), (75), (76) Contacts.
(80) Speed adjusting motor.
(81), (82) Relays.
(83), (84) Condensers.
(85) Resistor.

The device employed for frequency equalisation is shown in Fig. 3. Here the contact drum (71), which resembles a commutator with six segments, is affixed to one end of the shaft (33) of the synchronoscope. A brush holder (73) is carried on the shaft (33), but is free to rotate independently of the latter. The friction between the brush and the revolving contact drum causes the brush holder to be carried along with the latter until it is stopped by either contact spring (74) or (75). If the shaft (33) rotates in anti-clockwise fashion, electric impulses are passed to the relay (81) over the contact (76), the brush holder (73), the segments (72) of the contact drum (71), and the contact (74). Relay (81) is of the time-delay type, so that its contacts remain in the closed position if the impulse frequency exceeds a certain value. In this event, the speed adjusting motor (80) diminishes the speed of the turbine, hereby decreasing the difference in frequency between generator and bus. This decrease in the frequency difference results in a diminution in the frequency of the successive impulses impressed upon the coil of the relay (81), and the latter will therefore open the circuit of the speed adjusting motor (80).

If the speed of the generator is too low, shaft (33) will rotate in clockwise fashion, the brush holder (73) will be carried against contact point (75) and the connecting impulses will be transmitted to relay (82). Its operating principle is identical with that of relay (81), but with the difference that it serves to operate the speed adjusting motor (80) to increase the speed of the turbine.

TEMPERATURE MEASUREMENT OF AIR AND GASES AT HIGH VELOCITY OF FLOW.

By A. E. HINTERMANN. (From *Technische Rundschau*, Vol. 36, 1944, No. 30, pp. 1 and 2.)

A BODY neither receiving from nor yielding heat to an external source and exposed to a stream of air flowing at moderate velocity will assume the temperature of the air. However, at high air speeds of the order of the velocity of sound, its temperature will exceed that of the air. This temperature increase is due to the fact that the speed of the air impinging upon the body is reduced to zero, hereby increasing in temperature partly because of its pressure increase and partly because of its internal friction. A thermometer swept by a stream of high velocity air or gas will, therefore, indicate a temperature in excess of the true temperature of the air or gas. This temperature increase must be known if true air temperatures are to be determined in the investigation of blowers, compressors, or flow of conditions in conducts and pipes, wind tunnels, etc.

If t_{st} denotes the temperature corresponding to an assumed perfect adiabatic compression caused locally by the presence of the thermometer in the air stream, and if t_w denotes the true temperature of the air stream, then the temperature t_g indicated by the thermometer will lie between t_{st} and t_g. On the basis of adiabatic compression it is

$$t_{st} - t_w = \frac{V^2}{2g\,(k/k-1)\,R} = \frac{V^2}{2g} \cdot \frac{A}{c_p}$$

where V is the velocity of the air or gas, g is the gravitational constant, c_p is the specific heat of the air or gas at constant pressure, c_v that at constant volume K denotes the ratio c_p/c_v, R is the gas constant and A' is the mechanical heat equivalent.

Considering the case of air, it can be written

$t_{st} - t_w = \frac{V^2}{2{,}000}$ where $t_{st} - t_w$ corresponds to perfect adiabatic compression, which does not, however, obtain over the entire thermometer body. The temperature indicated will, therefore, lie below the theoretical value for t_{st}, so that the indicated temperature will equal

$t_g = t_w + \psi \frac{V^2}{2{,}000}$ where ψ is a coefficient which is smaller than unity. Tests have shown that values for ψ may range from 0.5–0.85, the actual value also largely depending upon the contour of the thermometer. If an ordinary precision thermometer is to be used, its actual ψ value will have to be determined by test. This determination of ψ will best be carried out as follows: It is $\psi = 1 - \frac{2000}{V^2}(t_{st} - t_g)$. By means of a blower of sufficiently large pressure ratio, air is drawn from a large air space in which the air has the temperature t_{st}, while V is the velocity of the air at the point of the suction duct where the thermometer is installed. The value of V prevailing can then be determined by means of the gas equation and with the use of an entropy table. With t_g denoting the temperature indicated by the thermometer, it is then possible to compute the value for ψ. The usefulness of this method is, however, impaired by the fact that, as experience has shown, the ψ values obtained are relatively widely scattered, thus causing errors of measurements.

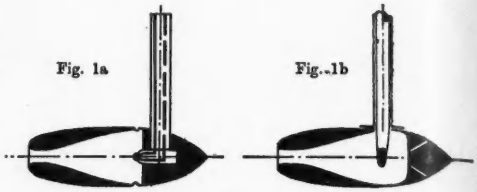

For the purpose of measuring directly the temperature t_{st}, the special instrument shown in Figs. 1*a*, 1*b* has been developed. This instrument is seen to incorporate a diffusor in which the velocity of the air stream impinging upon the instrument is reduced to a very small value, the temperature being measured at the point of lowest air speed. This reduction in flow velocity is made so great that the thermometer reading approximates to the air temperature. Lateral air impingement upon the instrument is of relatively small importance, angles of incidence of the air stream up to ±10 deg. being permissible. The only effect of such an angularity will be a diminution in the air flow passing through the instrument, but this will not affect the working principle. A thermometer of this type equipped with a thermocouple is outlined in Fig. 1*a*, while Fig. 1*b* shows an instrument incorporating a thermometer of the ordinary type. It will be noted that the cavity of the instrument is provided with small vents which ensure that at all times the correct gas temperature prevails in the interior.

Calibration of the instrument—that is to say, determination of the coefficient ψ,—is, of course, required, but its values are more consistent than is the case with the ordinary thermometer. Actually, the ψ value remains constant over a range from 50 to 250 m. per sec. velocity of flow. Numerically the coefficient ψ varies between 0.98 and 1.0, as compared to a range of 0.9–0.95 with the ordinary thermometer. The theoretical temperature rise with varying velocity of flow in the case of perfect adiabatic conditions is charted in Fig. 2, where it is seen that with a velocity V = 100 m. per sec. the temperature rise would amount to 5 deg. C. and reach 19.8 deg. C. with a flow velocity of 200 m. per sec.

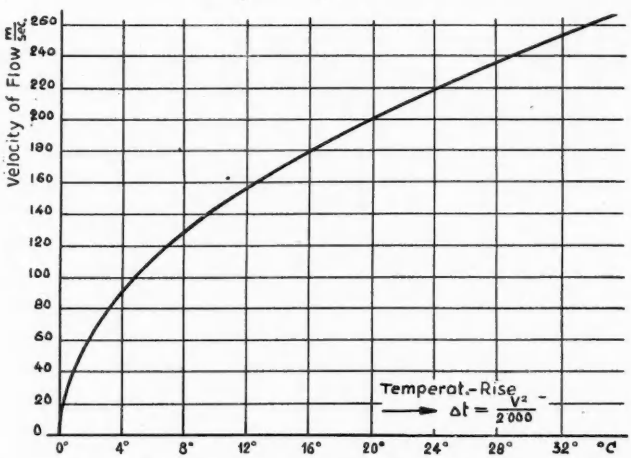

Fig. 2. Connection between the velocity of flow and the temperature rise in the case of perfect adiabatic conditions.